Leveraging De Donder relations for a thermodynamically rigorous analysis of reaction kinetics in liquid media

Thomas J. Schwartz[1] and Jesse Q. Bond[2]

1. Department of Chemical & Biomedical Engineering, University of Maine
2. Department of Biomedical & Chemical Engineering, Syracuse University

Abstract

This Mini-review considers the use of De Donder relations to facilitate a thermodynamically rigorous discussion of liquid phase reaction kinetics through the analysis of elementary steps. In quantifying "solvent effects," pure species reference states are convenient. Rate expressions developed with this convention capture all effects of thermodynamic non-ideality in solvent-specific activity coefficients or excess free energies, whereas commonly applied infinite dilution reference states lead to solvent- and composition-dependent standard-state rate and equilibrium constants. Two solvent effects are described: a "kinetic" effect, which comprises solvation of a transition state relative to reactants in an elementary step, and a "thermodynamic" effect, which comprises solvation of products relative to reactants in an elementary step. The former impacts the forward rate constant, and the latter impacts reversibility. These effects are formally encoded in De Donder rate expressions; thus, they inherently account for solvation while maintaining thermodynamic consistency with respect to elementary rate and equilibrium constants. A series of case studies are presented. These demonstrate that solvent effects can lead to substantial deviations from anticipated behavior during routine analysis of liquid-phase reactions. Additionally, we find that surface reactions and degree of rate control in multi-reaction sequences can be impacted by bulk solvation, but such effects are difficult to predict *a priori*.

Highlights

- Thermodynamically consistent rate laws are developed using De Donder relations.
- De Donder relations force thermodynamic rigor, so they are ideal for liquid-phase analysis.
- Pure species reference states are convenient when quantifying the impacts of solvent variation.
- Thermodynamic nonidealities may cause composition-dependent rate constants, leading to unexpected non-linearity in analysis.
- Solvation effects are non-trivial in multi-step reaction mechanisms.

1 Introduction

Catalytic processes in condensed media are important for a variety of emerging and established industries. Biorefining requires upgrading carbohydrates and lignin, which are thermally unstable macromolecules. Further, the platform chemicals derived therefrom—levulinic acid, γ-valerolactone, 5-hydroxymethylfurfural, and aromatic oxygenates—are oxygen-rich, polar, non-volatile, and reactive [1, 2]. These characteristics all demand low-temperature, solution-phase processing. In addition, the trend toward low-cost, carbon-free electricity makes electrochemical and electrocatalytic reduction attractive for a broad set of hydrogen-intensive processes, including CO_2 hydrogenation [3] and ammonia synthesis [4, 5]. The requirement of charge conduction dictates that electrochemical processes occur in a condensed phase [6].

The catalysis community has primarily focused on the design of new, increasingly complex materials to break longstanding performance plateaus. For reactions in condensed media, rational design of the solvent environment is equally important. Diversity in the chemical and physical structures of molecules allows for tunable interactions between solvents, solutes, and/or electrolytes, which can have profound impacts on reactivity and selectivity. Indeed, there are many examples where the solvent is more critical than the catalyst in determining feasibility. A classic example is the acid-catalyzed dehydration of fructose to form 5-hydroxymethylfurfural [7]. The reaction is Brønsted-mediated [8], and, while the literature reports numerous homogeneous [9–11] and heterogeneous proton sources [12, 13], they all perform comparably to the benchmark mineral acids that have been used to dehydrate sugars for the better part of a century (*e.g.*, HCl, H_2SO_4). As evidenced by work from Moreau [12], Dumesic [14, 15], Huber [16], Wyman [9], and others [17–19], far more significant gains in selectivity are attainable through solvent manipulation. Similarly, there has been extensive discussion of reactions, such as metal-catalyzed carbonyl hydrogenation [20, 21], acid-catalyzed alcohol dehydration [22–26], alkene epoxiation [27], and Fisher-Tropsch synthesis [28], that show remarkable rate enhancements in the presence of certain solvents. These "solvent effects" are evident at the macroscale, and their molecular-level impacts are well-developed in chemical thermodynamics. That said, there are few cases where the fundamental underpinnings of solvation have been correctly embedded in the analysis of liquid-phase reactions [7, 28–31]. Common practice is to process kinetics data using the machinery of transition state theory applied to *thermodynamically ideal* systems; however, this approach is inadequate for describing solvation, *which is a consequence of thermodynamic nonideality.*

Toward our goal of enabling the rational design of liquid-phase, catalytic processes, we outline a thermodynamically rigorous framework for the analysis of elementary and macroscopic reaction kinetics. We do so using the concept of reaction affinity, which was originally developed by De Donder [32, 33]. This method is ideally suited to a description of liquid phase reactions because it explicitly captures the impacts of solvation on elementary free energies of reaction and activation. Our presentation is inspired by concepts discussed in Denbigh's *The Principles of Chemical Equilibrium* [34]; Denbigh's and Turner's *Chemical Reactor Theory* [35]; Sandler's *Chemical and Engineering Thermodynamics* [36]; Laidler's *Chemical Kinetics* [37]; O'Connell's and Haile's *Thermodynamics: Fundamentals for Applications* [38]; *The*

Microkinetics of Heterogeneous Catalysis [39] and related articles by Dumesic [40–43]; the works on microkinetic analysis and degree of rate control by Campbell [44–47] and others [48–51]; the excellent paper from Madon and Iglesia on reactions in thermodynamically nonideal media [29]; and, of course, pioneering works by Michel Boudart [33, 52–55], wherein the development of rate expressions for thermodynamically non-ideal systems is addressed directly [56]. Importantly, it was Boudart's interest in the concept of reaction affinity that inspired the modern take on De Donder relations and Degree of Rate Control that has evolved over the last 30 years [40].

Readers familiar with the above references will recognize concepts herein, which are relatively well-established. That said, they are infrequently applied in catalysis practice, particularly in the experimental analysis of liquid-phase reactions. This is a consequence of entrenched conventions that take an overly simplified approach to the development of rate laws, which has implications in fundamental kinetic analysis. Our aim in this Mini-review is twofold. First, we hope to build an understanding of why conventional approaches have been historically successful but may fail for reactions in solution. Second, we aim to provide the community with a rigorous, yet tractable framework for the analysis of reactions in solution. De Donder relations address both goals. They are straightforward to develop, and, as one does so, solvation effects are clearly resolved and rigorously quantified. Accordingly, we tailor classic De Donder relations to liquid-phase reactions, and we apply them in the analysis of multiple case studies through which we highlight the unpredictable ways that solvation can impact elementary and macroscale phenomena. The discussion to follow presumes systems that are characterized by infinitely fast heat and mass transfer [57, 58] and are free from product inhibition [59]. Further, our primary focus is the solvation of reacting species by a bulk liquid; hence, we do not consider the potentially significant impacts of competitive solvent adsorption [60, 61] or lateral interactions [28]. Finally, it is important to state explicitly that De Donder relations and the rate expressions developed therefrom are strictly valid only for elementary steps. As we show in various case studies, one *can* use De Donder relations to build thermodynamically rigorous expressions for overall reaction rates [50, 51, 62]; however, this is best accomplished by considering the impacts of solvation on the elementary steps comprising the reaction mechanism.

2 Background

Our default methods of kinetic analysis usually invoke tacit assumptions about reference states and thermodynamic ideality; historically, this has been of little consequence. This is because foundational work in chemical and catalytic kinetics was largely performed in gas-phase systems at low pressure, where partial pressures are reasonable approximations for fugacities, and where we employ a universal thermodynamic reference state of a pure species at 1 bar. This is not the case for liquid-phase reactions, which require a careful treatment of thermodynamics. Unfortunately, gas-phase conventions prevail in most analyses, leading to a broad mischaracterization of liquid phase kinetics and thus the impacts of solvation. To highlight incongruities in common approaches, it is helpful to consider a thought experiment.

2.1 A Textbook Analysis of Elementary Kinetics?

We begin by considering an elementary, liquid-phase reaction:

$$A \rightleftharpoons 2B \tag{1}$$

The law of mass action is appropriate for an elementary step. Thus, one writes a rate expression by assuming the rate scales with species concentration, with the order for each species given by its stoichiometric coefficient:

$$r = k_f C_A - k_r {C_B}^2 \tag{2}$$

Because this is an elementary reaction, microscopic reversibility [63] requires that the difference between forward and reverse free energies of activation is equal to the free energy of reaction [53]. Thus, the values of forward and reverse rate constants are constrained by the value of the equilibrium constant:

$$\frac{k_f}{k_r} = K = \exp\left(\frac{-\Delta G^\circ}{RT}\right)_{\mathrm{P}=1\,\mathrm{bar}} \tag{3}$$

This constraint precludes independent specification of the forward rate constant, the reverse rate constant, and the reaction free energy for an elementary step. More subtly, it requires that the extent of reaction obtained by solving the material balance for an arbitrary reactor at an infinite residence time must equal the composition predicted by the relationship between the equilibrium constant and the thermodynamic activities of species participating in the reaction [35]:

$$K = \frac{{a_B}^2}{a_A} \tag{4}$$

These are manifestations of microscopic reversibility for an elementary step [42, 62], and they are useful for characterizing elementary kinetics. Thermodynamic data are relatively accessible for stable species (*i.e.*, free energies of formation or combustion), so calculation of reaction free energies is often straightforward. In contrast, thermodynamic data for transition states (*i.e.*, free energies of activation) are significantly harder to come by. Accordingly, when describing the kinetics of an elementary step, it is a good practice to impose this constraint by specifying only one rate constant—whichever is more computationally or experimentally accessible—and computing the other as a function of the equilibrium constant (*i.e.*, the free energy of reaction). We caution that this constraint cannot be generally applied to empirical rate laws that describe overall reactions, only to rate expressions for elementary steps.

$$k_r = \frac{k_f}{K} \tag{5}$$

As both authors have observed while teaching courses in microkinetic analysis, a problem arises if this value of the reverse rate constant, k_r, is substituted directly into the rate law posited above (Eq. 2). A thermodynamic equilibrium constant, K, is a dimensionless quantity. Thus, one consequence of microscopic reversibility is that forward and reverse rate constants in an elementary step must have identical units. In contrast, the mass action rate equation written in terms of species concentrations (Eq. 2) requires a first-order forward rate constant (with dimensions of inverse time) and a second-order reverse rate constant (with dimensions of inverse concentration and inverse time) for dimensional consistency.[1] This discrepancy becomes plainly visible when considering an arbitrary reactor at an infinite residence time, where the elementary step is equilibrated and its rate decays to zero. In this regime, we set the mass action rate law equal to zero , which gives the following result:

$$\frac{k_f}{k_r} = \frac{{C_B}^2}{C_A} \tag{6}$$

More fundamentally, for an elementary step at chemical equilibrium, microscopic reversibility requires that:

$$K = \frac{k_f}{k_r} = \frac{{a_B}^2}{a_A} \tag{7}$$

Equations 6 and 7 are in conflict, and they only reconcile for a reaction occurring in thermodynamically ideal media and for specific reference state conventions. In reality, the rate constants in Equation 6 and Equation 7 are fundamentally different, and they should not be conflated; unfortunately, common conventions in the specification of mass action rate equations tempt one to do so (as we have shown above).

We rarely discuss reference state conventions or the assumptions that underlie these default rate expressions, but these specifications are critically important. Failure to address them leads to significant complications, particularly in the analysis of liquid-phase systems. By stating that a liquid-phase reaction rate scales directly with species concentration, we are tacitly invoking results from Transition State Theory applied to a homogeneous reaction occurring in thermodynamically ideal media and for which thermodynamic data are specified at a hypothetical one-molar, solution-phase reference state that has infinite dilution properties. This may or may not be representative of the system under consideration; as such, our near-universal adoption of rate laws that presume thermodynamic ideality and an infinite dilution (1M) reference state is problematic. Consider the analysis of organic reactions, where one infrequently has access to thermodynamic data at infinite dilution in each solvent of interest. Data for pure species are far more abundant; accordingly, most of us compute thermodynamic functions that are based on pure species reference states. When

[1] It is worth considering that elementary rate constants developed using transition state theory, $k = \frac{k_b T}{h} exp\left(\frac{-\Delta G^{\ddagger}}{RT}\right)$, have units of inverse time regardless of reaction order. This is consistent with microscopic reversibility. As we demonstrate hereafter, dimensions of concentration appear in rate constants only after one sets an intensive basis, assigns reference states, and defines thermodynamic activities in transition state theory rate expressions.

we couple this with our tendency to write rate expressions as functions of concentration, we are mixing reference state conventions. This has serious consequences. Even in the rare case of a thermodynamically ideal liquid-phase reaction, mismatched reference states yield kinetic models that violate thermodynamic consistency. For the more common case where liquid media deviate from thermodynamic ideality, there is a complex relationship between composition and chemical potential. This can lead to unpredictable behavior, invalidate core assumptions, and obscure the fundamental origins of changes to the apparent, macroscale observables favored by experimentalists, *i.e.* rate constants, reaction orders, and activation barriers.

Concentration-based rate expressions have been successfully applied in the analysis of gas-phase reactions for decades. This hinges on two important details. First, for gas-phase systems, composition dependencies in rate and equilibrium expressions almost always reduce to partial pressures and a reference state of pure species at 1 bar. Second, for gases at low pressure, the assumption of thermodynamic ideality introduces little error. Even at considerable pressures, fugacity coefficients rarely show substantial deviations from unity. As a consequence, for most gas-phase reactions, *partial pressures provide a thermodynamically rigorous stand-in for fugacities*. For this reason, variations in gas-phase chemical potentials are well-described by variations in species partial pressure. This means that partial pressures (and thus concentrations) rigorously capture composition dependencies in rate and equilibrium expressions for gas-phase reactions. Further, the near-universal reference state convention of pure species at 1 bar means that thermodyanmic activities, free energies of reaction, and free energies of activation almost always use a common standard state, so thermodynamic consistency is easily ensured. Gas phase methodologies have come to define a standard approach for kinetic analysis; unfortunately, the above conveniences do not extend to liquid-phase systems, where one finds multiple reference state conventions and substantial deviations from thermodynamic ideality. Put simply, in liquid media, one can not generally trust that concentration is an adequate stand-in for chemical potential.

In a practical sense, describing liquid-phase kinetics using concentration-based rate expressions is useful. Concentrations are convenient to measure and control, whereas thermodynamically rigorous quantities (*i.e.*, activities, fugacities, and chemical potentials) are not. Furthermore, concentration-based rate expressions are generally adequate for applied problems in reactor design, where it is often unnecessary to resolve solution thermodynamics to correctly size or scale a reactor. However, liquid-phase processes are becoming more prevalent, and we have become increasingly interested in rational pairings of solvent and catalyst. As we seek to understand and leverage solvation, it is important that we move toward improving thermodynamic rigor in kinetic analysis. Unfortunately, this is non-trivial, and it is almost universally excluded from formal training in chemical kinetics. After years of struggling to define best practices, it was humbling for the authors to realize that De Donder provided an ideal framework nearly 100 years ago. De Donder's approach is perfectly suited to the analysis of liquid-phase reactions because it is based upon a comprehensive, fundamental treatment of kinetic and thermodynamic driving forces for elementary reactions. As such, De Donder relations enable a complete resolution of "solvent effects" and prevent mischaracterization of observable phenomena.

2.2 Chemical Potential, Activity, and Fugacity

Species chemical potential, μ_j, is the driving force for chemical reactions [38], and it appears in multiple steps of the derivations to follow. Accordingly, we need a framework for computing the chemical potential of a species in terms of measurable and tabulated quantities. This is done using Equation 8, which casts μ_j as a function of its chemical potential in a thermodynamically ideal reference state, G_j° (*i.e.*, its partial molar Gibbs free energy[2]), and a thermodynamic activity, a_j, which reflects a perturbation from the thermodynamically ideal reference state [34]. By inspection, we find that the activity of a species in its reference state, where $\mu_j = G_j^\circ$, is necessarily unity.

$$\mu_j = G_j^\circ + RT \ln (a_j) \tag{8}$$

Formally, the thermodynamic activity of a species in a mixture, a_j, is defined as the ratio of the fugacity of the species in the mixture, f_j, to the species in its reference state, f_j°, as shown in Equation 9 [36].

$$a_j = \frac{f_j}{f_j^\circ} \tag{9}$$

It is difficult to put a fine point on what liquid-phase fugacities *are*, but it is useful to discuss them for what they enable—rigorous quantification of thermodynamic activities and chemical potentials for species in real systems. Conventions for specifying the fugacity of a species in a mixture, f_j, and the fugacity of a species in its reference state, f_j°, are dictated by the phase of matter; the availability of thermodynamic data; and convenience. In general, fugacities are a product of a pressure (*e.g.*, a system pressure or a saturation pressure), a composition (*e.g.,* a mole fraction), and correction factors that account for deviations from thermodynamic ideality (*e.g.*, fugacity coefficients and activity coefficients). Standard definitions rely on dimensionless compositions and correction factors; as such, fugacities always have units of pressure. Importantly, by using fugacities to define thermodynamic activities (Eq. 9), one is forced to consider reference states, which helps to ensure thermodynamic consistency in rate expressions and De Donder relations. To this end, when defining a chemical potential, reference states used in calculating thermodynamic activities should be the same as those used in specifying standard state partial molar Gibbs free energies, G_j°. In the consideration of chemical reactions, reference states are typically specified at the temperature of the reacting system and a pressure of 1 bar; beyond this, there is considerable variation in reference state composition and state of matter. Some common reference states include pure gases; pure liquids; pure solids; and 1 molar or 1 molal solutions of dissolved solutes that have infinite dilution properties. Although Equations 8 and 9 make clear the necessity of defining fugacities and reference states, it is counterproductive to present an exhaustive list

[2]Note that chemical potentials are equivalent to partial molar Gibbs free energies. We prefer the use of the term "partial molar Gibbs free energies" for thermodynamically ideal reference states because these quantites are eventually collected into a Gibbs free energy change of reaction, which is the more familiar term in kinetic analysis. However, in most thermodynamics texts, Equation 8 uses the symbol μ_j° rather than G_j°.

of conventions here. We will instead focus our discussion on best practices in the characterization of solvent effects. For a general discussion of fugacities and thermodynamic activities, Sandler's *Chemical and Engineering Thermodynamics* is a good reference [36].

2.3 Thermodynamic Reference States

Before one can quantify activities and chemical potentials, it is necessary to define a thermodynamic reference state. Numerous conventions are in use [34, 36, 38], and as long as the same reference state is applied consistently throughout the analysis, one may choose any that is convenient. Unit molarity reference states (with infinite dilution properties) are often suggested for the analysis of condensed-phase reactions. This is the convention that most of us apply by default when we write concentration-based rate laws for liquid-phase reactions. In our view, this is a cumbersome reference state for consideration of solvent effects. Instead, we suggest that the pure species reference state is more useful in practice.

Infinite dilution reference states define systems that are dominated by solute-solvent interations and where solute-solute interactions are non-existent. These reference states are useful in cases where solute mole fractions can be maintained at or near the infinite dilution limit ($x_j \lesssim 0.01$) and *where the solvent identity is constant*. With this convention, activity coefficients are unity in the infinite dilution limit. Accordingly, as long as the system remains at infinite dilution, one can use concentration as a rigorous stand in for thermodynamic activity in the development of rate and equilibrium expressions. This is attractive because concentrations are experimentally convenient. Infinite dilution criteria, are, in general, easily met in low molecular weight solvents, like water, where it is possible to span a large range of solute concentrations without exceeding solute mole fractions of ≈ 0.01. While this reference state is frequently useful, there are problems with this convention in a fundamental analysis of solvation. Most importantly, unity activity coefficients do not mean that the chemical potentials of reactants, products, and transition states are invariant with changes in solvent identity at infinite dilution. Instead, solvent-induced changes in chemical potential are embedded in the infinite dilution reference state, which is inherently solvent-dependent in this convention. As such, standard state free energies of reaction and activation will vary among solvents, requiring one to redefine critical parameters, like equilibrium constants, with every change in solvent identity.

Although this approach is reasonable in principle, it introduces problems in practice. At a conceptual level, redefinition of the standard state with each new solvent is a subtle detail that is likely to be overlooked, thereby inviting misinterpretation. Further, thermodynamic state functions are not generally tabulated for species at infinite dilution in multiple solvents, which prevents straightforward computation of, *e.g.*, solvent-specific equilibrium constants at infinite dilution. Finally, although one can often constrain bench-scale experiments to infinite dilution, real processes may deviate significantly from this limit. Infinite dilution activity coefficients vary substantially from unity at high concentration, where solute-solute interactions dominate. Indeed, one cannot even guarantee that infinite dilution activity coefficients will equal unity at 1M because infinite dilution properties may not hold at this concentration—a 1M solution with infinite dilution properties is a purely hypothetical reference state. For these reasons, when using infinite dilution reference states, one must generally

define a separate family of solvent-specific activity coefficients alongside solvent-specific rate and equilibrium constants. In short, one does not escape thermodynamic non-ideality simply by choosing an infinite dilution reference state, and the convention loses its convenience when one considers changes in solvent identity and operation over large ranges of solute concentration, as is likely for organic reactions. For tangible examples, one might consider the significant variations in reactant and product concentration—and thus the solvation environment—as batch reactors proceed from low conversion to high conversion. Alternatively, large variations in solute concentration should be anticipated in experiments designed to measure apparent reaction orders. These are commonly performed in tubular reactors under differential conditions to avoid concentration gradients *across* the reactor; however, a reliable determination of reaction orders generally requires order-of-magnitude variation in bulk species concentration over the course of the experiment.

For several reasons, we prefer the reference state of a pure liquid at 1 bar. First, thermodynamic data are widely available for pure species at 1 bar, especially for organic molecules, which are our primary interest. Second, the pure species reference state is independent of solvent identity, making this a useful convention for characterizing the impact of solvent manipulation. As we will show subsequently, when using a pure species reference state, one defines a single standard state equilibrium and/or rate constant. Thereafter, all deviations from thermodynamic ideality are captured through solvent-specific activity coefficients, which are functions of excess Gibbs free energies [34]. Importantly, many common models for predicting activity coefficients are also based on pure-species reference states (*e.g.*, UNIFAC [64]). In this convention, activity coefficients can vary by orders of magnitude at infinite dilution, and they approach unity for pure species. To develop a sense of scale for the impact of varying activity coefficients, consider that the UNIFAC activity coefficient for 2-pentanone dissolved in water at infinite dilution—a highly nonideal environment—is ≈ 100. In contrast, its activity coefficient in 1,4-dioxane at infinite dilution—a relatively ideal environment—is ≈ 1.

With the reference state of a pure liquid at 1 bar established, one defines fugacities and thermodynamic activities as in Equations 10 to 12 [38]:

$$f_j^\circ = P_j^{\text{sat}} \tag{10}$$

$$f_j = \gamma_j x_j P_j^{\text{sat}} \tag{11}$$

$$a_j = \frac{f_j}{f_j^\circ} = \gamma_j x_j \tag{12}$$

In the above, f_j° is the fugacity of species j in its reference state (pure liquid, 1 bar); f_j is the fugacity of species j at the system temperature, pressure, and composition; a_j is the thermodynamic activity of species j at the system temperature, pressure, and composition; x_j is the liquid-phase mole fraction of species j at the system temperature, pressure, and composition; γ_j is the activity coefficient for species j at the system temperature, pressure,

and composition; and P_j^{sat} is the saturation pressure of species j at the system temperature. These definitions assume that the reference pressure (1 bar) and the system pressure are sufficiently close to the saturation pressure of species j that one can neglect the Poynting correction. At modest pressures, this generally introduces little error for liquids, which have relatively small molar volumes.

3 The De Donder Relation

We now apply the above described reference state conventions and definitions for fugacities, activities, and chemical potentials to develop thermodynamically rigorous rate expressions using De Donder relations. In the De Donder framework, the net rate of an elementary step, r, is written in terms of the forward rate of reaction, r_f, and an "affinity" for the reaction, A [40],

$$r = r_f \left[1 - \exp\left(\frac{-A}{RT}\right)\right] \tag{13}$$

The first term, r_f, represents a purely kinetic term, *i.e.*, the rate of reaction that is attained at infinite displacement from chemical equilibrium. This can be derived using transition state theory. The second, bracketed term captures the thermodynamic driving force for the reaction. It comprises the gradient in free energy between the system at its present composition and the system at chemical equilibrium, where the reaction rate falls to zero. We find it helpful to consider the derivation in parts, and so we address each term separately.

3.1 The Forward Rate of Reaction: Kinetic Effects of Solvation

First, we develop a rate expression for the forward reaction using Transition State Theory. We pursue this development for a straightforward case: a unimolecular, irreversible, elementary reaction occurring homogeneously in condensed media. That said, the concepts are easily generalized to any system of interest (See Appendix B).

$$A \longrightarrow B \tag{14}$$

The rate of an elementary step—in extensive units—scales with the number of transition states present in the system [37]. Specifically, the extensive rate can be expressed as the product of the frequency at which the transition state is converted into products, $\nu^{\ddagger}$, and the number of transition states that exist in the system of interest, $N^{\ddagger}$.

$$\bar{r}_f = \nu^{\ddagger} \cdot N^{\ddagger} \tag{15}$$

An intensive rate expression is more useful in practice; however, by beginning from Equation 15 we are forced to consider an appropriate dimensional normalization. This ultimately leads

to straightforward development of rate expressions that are both rigorous and dimensionally-consistent. The basic tenets of transition state theory were developed in consideration of homogeneous reactions that occur uniformly in 3-dimensional space, leading to normalization of rates by volume [65]. This is reflected in the prevailing notion that reaction rates scale with the concentration of the transition state. Although a subtle point, it is perhaps more correct to state that the intensive rate of reaction *per unit volume* scales with the concentration of the transition state. One is free to chose any normalization that is convenient, which can allow, for example, a straightforward TST derivation for turnover frequencies in surface reactions (See Appendix B). Because we are presently considering a homogeneous, liquid-phase reaction (Eq. 14), we *choose* to normalize by system volume. This leads to the familiar starting point for the development of elementary rate expressions via Transition State Theory (Eq. 16).

$$r_f = \nu^{\ddagger} \cdot C^{\ddagger} \tag{16}$$

Here, $C^{\ddagger}$ represents the molar concentration of the transition state. Subsequently, one assumes that the transition state is in equilibrium with the reacting species that form it, with the system composition described by an equilibrium constant:

$$K^{\ddagger} = \prod_j a_j^{\nu_j} \tag{17}$$

Activities are defined as in Eq. 12, and the mole fraction of the transition state is described as a function of its concentration, $C^{\ddagger}$, the system volume, V, and the total number of moles, N:

$$x^{\ddagger} = \frac{C^{\ddagger} V}{N} \tag{18}$$

Thus, the transition state concentration can be expressed as a function of a thermodynamic equilibrium constant, a ratio of activity coefficients, the total bulk system concentration (*i.e.*, N/V), and a reactant mole fraction:

$$C^{\ddagger} = K^{\ddagger} \cdot \frac{\gamma_A}{\gamma^{\ddagger}} \cdot \frac{N}{V} \cdot x_A \tag{19}$$

Substituting this result into Eq. 16 yields the following expression:

$$r_f = \nu^{\ddagger} \cdot K^{\ddagger} \cdot \frac{\gamma_A}{\gamma^{\ddagger}} \cdot \frac{N}{V} \cdot x_A \tag{20}$$

In transition state theory, the equilibrium constant, $K^{\ddagger}$, is expressed as the product of a single, low-frequency vibrational mode and the standard state free energy change to form the transition state from the reactants:

$$K^{\ddagger} = \frac{k_B T}{h\nu^{\ddagger}} \cdot \exp\left(\frac{-\Delta G^{\circ,\ddagger}}{RT}\right) \tag{21}$$

Application of Eq. 21 then gives the transition state theory rate expression for an irreversible, unimolecular, elementary, liquid-phase reaction (Eq. 22), analogous to those developed elsewhere [26, 29, 31, 37].

$$r_f = \frac{k_B T}{h} \exp\left(\frac{-\Delta G^{\circ,\ddagger}}{RT}\right) \cdot \frac{\gamma_A}{\gamma^{\ddagger}} \cdot \frac{N}{V} \cdot x_A \tag{22}$$

Note that compositions are expressed here as mole fractions rather than concentrations, which is a consequence of our decision to work with pure species reference states. Upon seeing the product of x_A and N/V in the rate expression, it is tempting to replace it with C_A. However, this is a unique result for first-order reactions. When using a pure species reference convention, mole fractions cannot be replaced with concentrations for, *e.g.*, an elementary bimolecular reaction.[3] The free energy of activation, $\Delta G^{\circ,\ddagger}$, represents the standard state free energy change incurred upon converting the reactants as pure species into the transition state as a pure species. It is therefore independent of solvent identity. For this reason, we define a standard state rate constant, k°, whose value remains constant for any solvent and any degree of thermodynamic non-ideality (note, this is the same formalism adopted in the classical Brønsted-Bjerrum relation for consideration of ionic systems [35, 37]).

$$k^{\circ} = \frac{k_B T}{h} \cdot \exp\left(\frac{-\Delta G^{\circ,\ddagger}}{RT}\right) \tag{23}$$

It is worth pointing out that because k° is referenced to pure species, it is relatively easy to estimate its value using either computational methods or generalized correlations. In contrast, calculating the analogous free energy of activation for a solution-phase reference state requires one to explicitly consider solute-solvent interactions. Combining Equations 22 and 23 results in a concise, thermodynamically rigorous expression for the forward rate of reaction in condensed media.

$$r_f = k^{\circ} \frac{\gamma_A}{\gamma^{\ddagger}} \cdot \frac{N}{V} \cdot x_A \tag{24}$$

Because we have retained activity coefficients, this expression applies for any condensed-phase, homogeneous, unimolecular *elementary* reaction, regardless of solvent identity or degree of thermodynamic non-ideality. Solvation effects are embedded in the activity coefficients, which are specific to each solvent. This expression will capture any *"kinetic"* impact of solvation, *i.e.*, a solvent-induced change in the free energy separation between the transition state and the reactant state. From an experimentalist's perspective, the use of activity

[3] To develop a rate expression strictly as a function of species concentrations, one would instead employ a unit molarity reference state in developing Equations 17 to 20.

coefficients in Eq. 24 is convenient because of the broad availability of activity coefficient models (*e.g.*, Margules [36], Wilson [66], NRTL [67], UNIFAC [64], etc.). From a theoretician's perspective, these equations are probably better expressed solely in terms of Gibbs free energies, which are directly accessible through density functional theory or *ab initio* molecular dynamics simulations. The result is generalized by expressing activity coefficients as functions of excess Gibbs free energies, which are both solvent- and composition-dependent [34]:

$$\gamma_j = \exp\left(\frac{G_j^E}{RT}\right) \tag{25}$$

In this Mini-review, we primarily discuss activity coefficients since they are more concise, but, as Eq. 25 shows, these are interchangeable with excess Gibbs free energies. By substituting Eq. 25 into Eq. 22, we find that the ratio of activity coefficients, $\gamma_A/\gamma^\ddagger$, reduces to a change in excess Gibbs free energies of activation, $\Delta G^{E,\ddagger}$, leading to an equivalent rate expression:

$$r = \frac{k_b T}{h} \exp\left(\frac{-\left(\Delta G^{0,\ddagger} + \Delta G^{E,\ddagger}\right)}{RT}\right) \cdot \frac{N}{V} \cdot x_A \tag{26}$$

If one retains activity coefficients (Eq. 24), it is clear that, to observe a solvent effect, the activity coefficient ratio, $\gamma_A/\gamma^\ddagger$, must deviate from unity. This ratio reflects the degree of stabilization or destabilization of the transition state *relative to the reactants* (or, importantly, vice versa), which is another way of saying that the change in excess free energy of activation, $\Delta G^{E,\ddagger}$, is non-zero (Eq. 26). Stabilization of the transition state relative to the reactant ($\gamma_A/\gamma^\ddagger > 1$) will lead to an increase in the observed rate constant, whereas destabilization of the transition state relative to the reactant ($\gamma_A/\gamma^\ddagger < 1$) will lead to a decrease in the observed rate constant. Equivalently, Eq. 26 shows that a positive excess free energy of activation results in an increased free energy separation between the transition state and the reactant state, and a negative excess free energy of activation implies the converse. The former manifests as a decrease in the observed rate constant (lower "reactivity"), while the latter will increase the observed rate constant (higher "reactivity").

Because transition states are often chemically similar to the reactants that form them, it is reasonable to expect that the reactant and transition state will have similar activity coefficients [29]. In this case, even if individual activity coefficients deviate substantially from unity, no significant "kinetic" effect of solvation is observed because $\Delta G^{E,\ddagger}$ is approximately zero. For a solvent to perturb a rate constant, there must be a significant difference in the extent of solvation between reactants and transition states, which is anticipated only in systems where the two states are chemically dissimilar and there are strong interactions with the solvent. For example, one might anticipate a significant kinetic effect of solvation in an elementary step that proceeds through a late transition state and converts a polar reactant into a non-polar product.

3.2 The Net Rate of Reaction: Thermodynamic Effects of Solvation

Equations 24 and 26 apply only to an elementary step that is infinitely displaced from chemical equilibrium. As the system approaches chemical equilibrium, the reverse reaction becomes significant, and the net rate of reaction decreases relative to the aforementioned limit. This is best described as a decrease in the *thermodynamic* driving force for reaction, and it can also be impacted by solvation. Rigorously capturing these impacts is where De Donder relations truly shine.

We begin by relaxing the assumption of irreversibility in our homogeneous reaction:

$$A \rightleftharpoons B \tag{27}$$

In the preceding section, we derived a rate expression for the forward reaction using Transition State Theory and pure species reference states (Eq. 24). We now substitute that expression into the De Donder relation (Eq. 13), which gives the net rate of reaction:

$$r = k^{\circ}\frac{\gamma_A}{\gamma^{\ddagger}} \cdot \frac{N}{V} \cdot x_A \left(1 - \exp\left(\frac{-A}{RT}\right)\right) \tag{28}$$

The parenthetical quantity on the right hand side captures the thermodynamic driving force for the reaction. The exponential term is generally called the "reversibility" of the reaction. For convenience, it is assigned the symbol z [40]:

$$z = \exp\left(\frac{-A}{RT}\right) \tag{29}$$

The reaction affinity, A, is defined as the negative change in the system Gibbs free energy, G, with respect to the extent of reaction, ξ, with temperature and pressure held constant at reaction conditions [53]:

$$A = \left(\frac{-\partial G}{\partial \xi}\right)_{T,P} \tag{30}$$

Following standard thermodynamic definitions for the total derivative of $G(n, P, T)$, this partial derivative is defined in terms of chemical potentials for each species, μ_j (Eq. 31). Substituting the definition of chemical potential (Eq. 8) allows this summation to be expressed in terms of standard state partial molar Gibbs free energies, G_j°, and thermodynamic activities of reactants and products as they exist under reaction conditions, a_j.

$$A = -\sum_j \nu_j \mu_j = -\sum_j \nu_j \left[G_j^{\circ} + RT\ln(a_j)\right] \tag{31}$$

The first summation on the right hand side is equal to the standard state free energy of reaction, which leads to a practical expression for reversibility:

$$z = \frac{\prod_j a_j^{\nu_j}}{\exp\left(\frac{-\Delta G^\circ}{RT}\right)} \tag{32}$$

Importantly, the standard state free energy of reaction as we have defined it reflects the conversion of reactants as pure species into products as pure species. Similar to the standard state rate constant, k°, described in the preceding section, it is not impacted by composition or solvent identity. Accordingly, we define a standard state equilibrium constant, K°, which is unaffected by changes in composition or solvent environment. This gives a concise expression for reversibility:

$$z = \frac{\prod_j a_j^{\nu_j}}{K^\circ} \tag{33}$$

Substituting Eq. 33 into the De Donder rate expression (Eq. 28) yields the following form, which makes clear some important limiting behavior.

$$r = k^\circ \frac{\gamma_A}{\gamma^\ddagger} \cdot \frac{N}{V} \cdot x_A \left(1 - \frac{\prod_j a_j^{\nu_j}}{K^\circ}\right) \tag{34}$$

First, $\prod_j a_j^{\nu_j}$ is equal to zero at infinite displacement from chemical equilibrium, where product mole fractions are zero. This ensures that the thermodynamic driving force for reaction is at a maximum value of 1 when the system is infinitely displaced from chemical equilibrium (*i.e.*, $z = 0$). Accordingly, in this limit, one observes the maximum possible net rate of reaction, which is equal to the rate of the irreversible forward reaction. Second, this expression guarantees that the rate of reaction decays to zero at chemical equilibrium, where $K^\circ = \prod_j a_j^{\nu_j}$. In this way, the De Donder relation rigorously enforces constraints on an elementary step that arise from microscopic reversibility. We next expand the components of the reversibility, z, which highlights the impacts of solvation on reaction affinity. We again express thermodynamic activities as functions of activity coefficients and mole fractions, per Eq. 12:

$$r = k^\circ \frac{\gamma_A}{\gamma^\ddagger} \cdot \frac{N}{V} \cdot x_A \left(1 - \frac{1}{K^\circ} \frac{\gamma_B}{\gamma_A} \frac{x_B}{x_A}\right) \tag{35}$$

Because we retain activity coefficients, the rate expression given in Eq. 35 applies in condensed media regardless of solvent identity or degree of thermodynamic nonideality; moreover, it explicitly accounts for displacement from chemical equilibrium. In this full rate expression, there are two ratios of activity coefficients that describe the impacts of solvation. As before, the kinetic impact of solvation is captured by the ratio $(\gamma_A/\gamma^\ddagger)$. Here, we

also see a "thermodynamic" impact of solvation, captured by the ratio (γ_B/γ_A). We clarify these impacts by expressing rate constants, equilibrium constants, and activity coefficients as functions of Gibbs free energy. Per convention, we define $\Delta G^{E,\ddagger}$ as the change in excess Gibbs free energy of activation, and we define ΔG^E as the change in excess Gibbs free energy of reaction. Standard state free energies of activation, $\Delta G^{\circ,\ddagger}$, and reaction, ΔG°, are based on pure species reference states and are thus independent of composition and solvent identity, while excess Gibbs free energies of reaction and activation are composition- and solvent-dependent, so $\Delta G^{E,\ddagger}$ and ΔG^E in Eq. 36 have implicit composition dependencies.

$$r = \frac{k_b T}{h} \exp\left(\frac{-\left(\Delta G^{0,\ddagger} + \Delta G^{E,\ddagger}\right)}{RT}\right) \frac{N}{V}\, x_A \left(1 - \frac{x_B}{x_A} \exp\left(\frac{\Delta G^0 + \Delta G^E}{RT}\right)\right) \tag{36}$$

If the presence of a solvent induces a non-zero excess free energy of activation (*i.e.*, $\Delta G^{E,\ddagger} \neq 0$), one will observe a perturbation to the observed rate constant and thus a "kinetic" impact of solvation. Alternatively, a solvent will have a "thermodynamic" impact when solvation induces a change in the reaction free energy (*i.e.*, $\Delta G^E \neq 0$). This will generally cause a change in the equilibrium position of the affected elementary reaction, which manifests in two important ways. First, it will change the equilibrium extent of reaction. For example, one might observe different equilibrium concentrations or coverages of an intermediate that has been stabilized or destabilized by solvation. Second, because the excess free energy of reaction appears in the reversibility, it will change the thermodynamic driving force for reaction, $(1-z)$. This results in a different reaction rate at an identical extent of reaction, even in the case where forward rate constants are identical. Generally speaking, a positive excess Gibbs free energy of reaction will decrease the thermodynamic driving force for reaction, while a negative excess Gibbs free energy of reaction will increase the thermodynamic driving force for reaction.

Solvent-induced perturbations to reaction free energies are anticipated where reactants are chemically distinct from products and there are strong interactions between solutes and solvents. Whereas transition states are frequently similar to reactant states, product states and reactant states often vary in terms of structure, functional groups, and polarity. This suggests that reactants and products are likely to have unique susceptibilities to solute-solvent interactions and that free energies of reaction may be generally more sensitive to solvation than free energies of activation. That is to say, manipulation of the solvent seems more likely to have a "thermodynamic" impact than a "kinetic" impact on a given elementary step. Although kinetic studies are usually performed under differential conditions where the *overall reaction* is far from equilibrium, one generally assumes that the majority of elementary steps in the underlying reaction mechanism are quasi-equilibrated and that multiple equilibrium constants are embedded in the overall rate expression. As such, the thermodynamic effects of solvation on individual elementary steps may be significant under conditions where the overall reaction is kinetically controlled, provided that the affected equilibrium constant appears in the overall rate expression.

We next demonstrate application of rate laws developed through the De Donder formalism in various case studies. In each, we highlight potential impacts of solvation, and we comment

on the ways that they might manifest and the implications for experimental design.

4 Case Studies

4.1 An Irreversible, Elementary Reaction

Even in simple systems, solvation can have surprisingly complex impacts. It is worth considering these scenarios as they build a foundation for more complex analysis, and they inform our expectations about how changes in solvent identity and species composition may influence reacting systems. For now, we consider the irreversible elementary step:

$$A \longrightarrow B$$

4.1.1 Variable Rate Constants: A Kinetic Impact of Solvation

In common experimental practice, one would assume that the rate of the elementary step $A \longrightarrow B$ will scale directly with composition and thus take the form:

$$r = k' \cdot \frac{N}{V} \cdot x_A \tag{37}$$

A comparison of this empirical rate expression with those derived directly from Transition State Theory (Equations 24 and 26) suggests two equivalent expressions for the apparent rate "constant" in a typical, composition-based rate expression, k'. Eq. 38 thus captures "kinetic" impacts of solvation, which manifest as changes in the observed rate constant for a given elementary step.

$$k' = \begin{cases} k^\circ \frac{\gamma_A}{\gamma^\ddagger} \\ \\ \frac{k_b T}{h} \exp\left(\frac{-\left(\Delta G_j^{0,\ddagger} + \Delta G_j^{E,\ddagger}\right)}{RT}\right) \end{cases} \tag{38}$$

It is critical to recognize that, although the standard state free energy of activation is composition-independent, (*i.e.,* k° is composition-independent), excess free energies of activation (and thus activity coefficients) have strong, nonlinear composition dependencies. Therefore, one should anticipate that the observed rate "constant" in a composition-based rate equation, k', is not only solvent-dependent, but also *composition dependent within that solvent*. This has implications for characterizing the rate of reaction along a reaction coordinate, where one generally observes large changes in species composition.

It now becomes essential to estimate values for activity coefficients, and to capture their variations with system composition. For simplicity, we utilize a single parameter Margules model to do so (Eq. 39)[36]. This is a truncation of the Redlich-Kister expansion, and it quantifies excess Gibbs free energies relative to a pure-species standard state. It is a univariate function of solvent mole fraction, x_S, and it is parameterized with a single, composition-independent

coefficient, $\Lambda_{j,S}$, that reflects the solvation of species j in solvent S [36, 38]. Specifically, a comparison with Eq. 25 reveals that $\Lambda_{j,S}$ is equal to $G^{E,j}/RT$ for species j in solvent S at infinite dilution, where $x_S = 1.0$. The one-parameter model is accurate for simple mixtures, but it can fail when higher-order, asymmetric non-idealities exist and more complex solution models are required. Regardless, it is adequate for illustrating salient points, and the following concepts are easily generalized to more sophisticated solvation models as required for real systems.

$$\ln(\gamma_j) = \Lambda_{j,S} \cdot {x_S}^2 \tag{39}$$

To visualize the impact of a composition-dependent rate constant, we consider the case of the unimolecular, irreversible elemenary step, $A \longrightarrow B$, wherein the reaction product, B acts as a selective solvent for the transition state, $A^{\ddagger}$. The transition state here can be either stabilized ($\ln(\gamma^{\ddagger}) < 0$) or destabilized ($\ln(\gamma^{\ddagger}) > 0$) relative to the reactant, A, which is not solvated ($\ln(\gamma_A) = 0$). Results are presented in Figure 1, where we illustrate the magnitude of the observed rate constant, k', as a function of solvent mole fraction, x_B, for three cases: one of an ideal solution ($\Lambda_{\ddagger,B} = 0$), one with a stabilized transition state ($\Lambda_{\ddagger,B} = -2$), and one with a destabilized transition state ($\Lambda_{\ddagger,B} = 2$). The observed rate constant was calculated using Eq. 38, and activity coefficients were calculated for the transition state in each solvation environment using Eq. 39. This range of Margules parameters corresponds to activity coefficients that range from $-2.0 \leq \ln(\gamma^{\ddagger}) \leq 2.0$ as a function of solvent mole fraction. To provide a connection to physically intuitive quantities, we note that extrema in this activity coefficient range are equivalent to changes in excess Gibbs free energies of activation of approximately ± 5 kJ mol^{-1} at 300 K. Although we present normalized rate constants in Figure 1, for the sake of completeness, the standard state rate constant, k°, was fixed at 1.0, and both it and the apparent rate constant, k', have dimensions of inverse time.

When the solvent mole fraction is 0 (*i.e.*, when the extent of reaction is zero), the system is thermodynamically ideal (pure A), and the observed rate constant, k', is equal to the standard state rate constant, k°, regardless of the value of the Margules parameter. Deviations from thermodyanmic ideality increase with solvent mole fraction (*i.e.*, as the reaction progresses). This causes the transition state to experience solvation relative to the reactant, and the observed rate constant increasingly deviates from the standard state value. As $x_B \rightarrow 1.0$, the transition state mole fraction approaches the infinite dilution limit, where pure species activity coefficients reach maximum deviation from unity. As anticipated in consideration of Eq. 38, stabilization of the transition state manifests as an increase in the observed rate constant, and we see the converse for destabilization. Importantly, we find that a relatively minor perturbation in the free energy of activation ($\pm \approx 5$ kJ/mol at 300K) causes order-of-magnitude variation in the observed rate constantover this composition range. This is reasonable considering that rate constants depend exponentially on activation barriers. One concludes that if preferential solvation of the transition state occurs to an appreciable extent, it should be readily apparent in a well-designed experiment.

This simple illustration shows that, in liquid media, rate "constants" may vary with solvent identity, composition, and even reaction progress. The extent of this variation will be de-

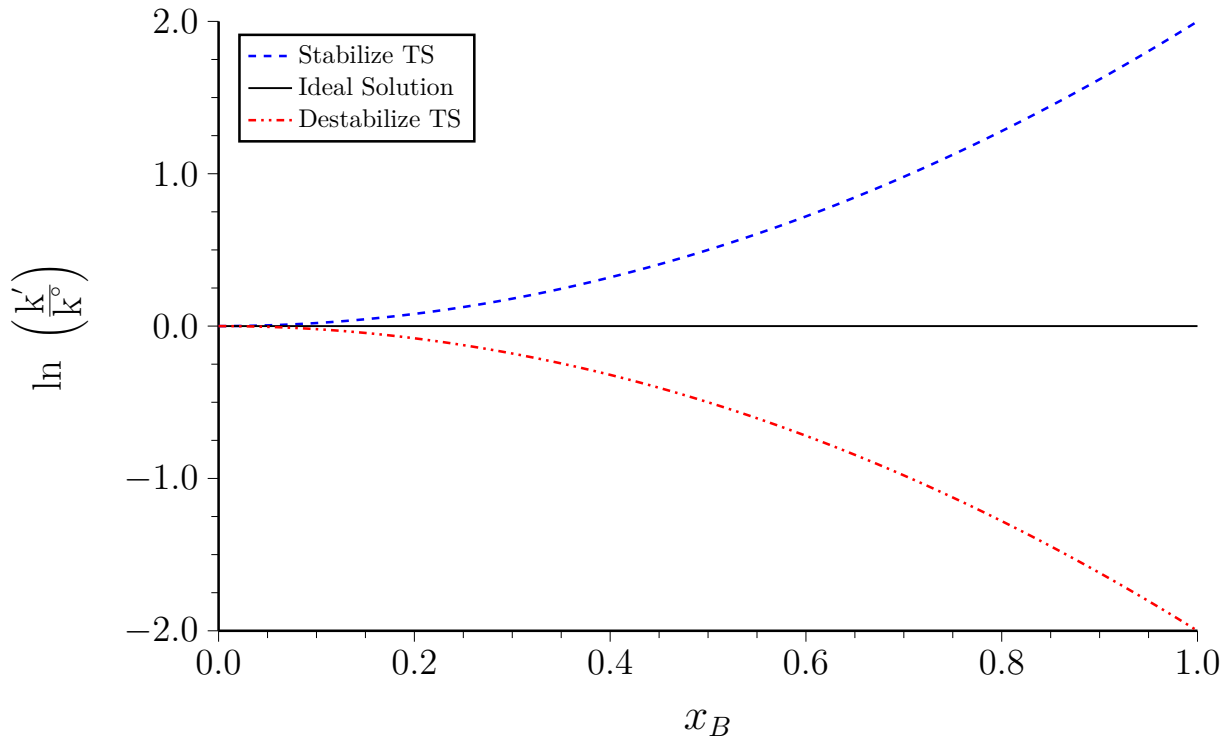

Figure 1: Impacts on observed rate constants of transition state solvation by reaction products, illustrating substantial deviation from ideality as fractional conversion increases. Ideal Solution, $\Lambda_{\ddagger,B} = 0$ (——); Stabilize Transition State, $\Lambda_{\ddagger,B} = -2$ (– – –); Destabilize Transition State, $\Lambda_{\ddagger,B} = 2$ (– · · –).

termined by the relationship between activity coefficients and composition over the range where data are collected. This is significant since our prevailing notion is that rate constants are independent of composition, and experimentalists rarely take measures to ensure composition-independent activity coefficients over the course of reaction progress.

4.1.2 Reactivity in Liquid-phase Batch Reactors

A composition-dependent rate constant may lead to complex behavior. We highlight potential issues by simulating the $A \longrightarrow B$ reaction in a constant-volume batch reactor that is initially charged with pure species A. We choose a constant-volume batch reactor as this is, by far, the most common system employed for the experimental characterization of liquid-phase reaction kinetics. Since we are considering an irreversible, elementary reaction, the rate is given by Eq. 24, where k° has a value of 1.0 in units of inverse time. The same solvent effects outlined above are used again here. Specifically, the reaction product B solvates the transition state, $A^\ddagger$, and we use Margules coefficients of -2.0, 0.0, and 2.0 with Eq. 39 to capture solvation of the transition state as a function of reaction progress. Results are presented in Figure 2. In general, solvation always results in deviation from the behaviors we anticipate for a first-order reaction in a constant-volume batch reactor. The consequences of this aberrant behavior are significant. For example, if the transition state is stabilized by solvation, the rate constant increases as a function of fractional conversion (Figure 1). This

increase mitigates the impact of decreasing reactant mole fraction, so the reaction rate decays more slowly than in the thermodynamically ideal system (Figure 2a), and the reaction reaches completion on significantly shorter time scales (Figure 2b). Destabilization of the transition state has the opposite effect.

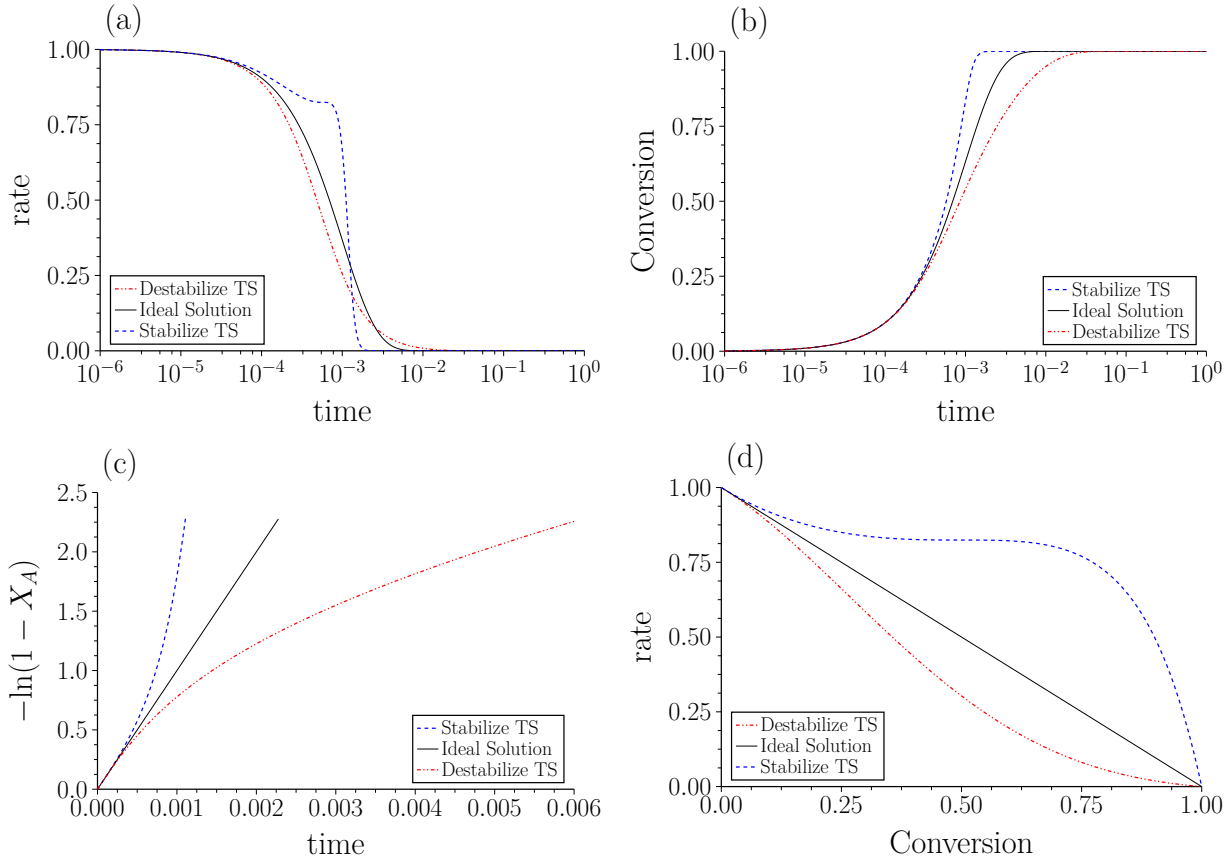

Figure 2: Impacts of transition state solvation in a constant volume batch reactor on reaction rate (a), fractional conversion (b), and common tests for first-order behavior (c and d). Ideal Solution, $\Lambda_{\ddagger,B} = 0$ (——); Stabilize Transition State, $\Lambda_{\ddagger,B} = -2$ (– – –); Destabilize Transition State, $\Lambda_{\ddagger,B} = 2$ (– · · –).

These composition-driven changes in rate constant are conceptually similar to those observed for adiabatic reactors where $\Delta H \neq 0$, which has significant implications for how we interpret the observed data. For example, a common analysis applied when studying first-order systems is to plot $-\ln(1 - X_A)$ against time (Figure 2c, X_A = fractional conversion) or rate against fractional conversion (Figure 2d), both of which should be linear. However, when the product appreciably solvates the transition state, one observes nonlinearity due to the rate constant's implicit composition dependence. Although this is a hypothetical scenario, these observations illustrate that common assumptions about reactor behavior may not hold for condensed-phase systems. Classical treatments generally presume a composition-independent rate constant, but this may be difficult to guarantee for reactions in solution, especially those carried out over large conversion ranges. This is important to consider since batch reactors are applied frequently in the study of liquid-phase reactivity, we often accumulate substantial fractional conversions therein, and we rarely ask the question of whether

or not rate constants vary with composition over the course of the experiment.

4.1.3 Experimental Determination of Reaction Orders

The potential composition dependence of the apparent rate constant, k', has serious implications for the determination of reaction orders in condensed media. Observed reaction orders are useful in kinetic analysis as they provide clues to the mechanism and rate determining step. Accordingly, one might consider measuring reaction orders in multiple solvents as a way to probe the impacts of solvation. In doing so, our usual approach would be modulate the substrate *concentration* in the solvent over several orders of magnitude; unfortunately, mole fractions are a better predictor of excess Gibbs free energies. The relationship between concentration and mole fraction is strongly solvent dependent, and one rarely has an intuitive sense of infinite dilution limits in molarity units.[4] A lack of awareness about infinite dilution limits may lead to unintended operation in regimes where activity coefficients (and thus rate constants) are strongly composition-dependent. This is especially problematic when comparing reaction kinetics in low molecular weight solvents, like water, to those observed in high molecular weight solvents, like hexadecane.

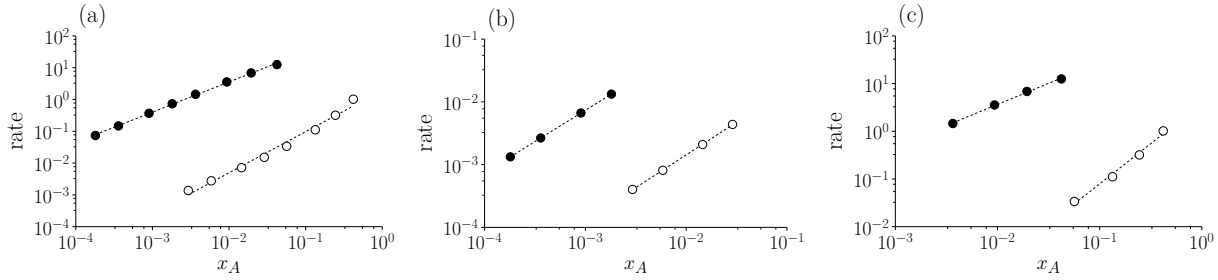

Figure 3: Impacts of transition state solvation on apparent reaction orders, showing a) non-linear behavior for a high-molecular-weight solvent (hexadecane, ○) and linear behavior for a low-molecular-weight solvent (water, •) over a concentration range of 0.01M to 2.0M, b) correct reaction orders obtained close to the infinite dilution limit ($C_j \leq 0.1$M), and c) deviations from the correct reaction order as one exceeds the infinite dilution limit ($C_j \geq 0.2$M).

To illustrate these effects, we plot reaction rates as a function of reactant mole fraction at zero conversion for the irreversible, elementary, unimolecular reaction $A \longrightarrow B$ occurring in water and hexadecane at concentrations ranging from 0.01 to 2.0 moles per liter (Figure 3). This set of concentrations mimics a typical span of experimental concentrations in liquid-phase kinetic studies. Rates were computed using Eq. 24, the standard state rate constant, k°, was fixed at 1.0 with dimensions of inverse time, and we used the single parameter Margules model (Eq. 39) for predicting activity coefficients for the transition state, $\gamma^\ddagger$, in each solvent, S. To facilitate contrast in the predicted reaction rates in Figure 3, we arbitrarily assume that water stabilizes the transition state ($\Lambda_{\ddagger,W} = -2.0$) and that hexadecane destabilizes it ($\Lambda_{\ddagger,H} = 2.0$). For the purpose of relating concentrations to reactant mole fractions, we assume that the reactant has properties of 2-butanol and that volume change of mixing is negligible. Data are presented on a log scale, so slopes of the regressed lines correspond to apparent reaction

[4] It is important to be aware of the infinite dilution limit since it defines a regime where activity coefficients are composition-independent.

orders. In water, one observes reasonable linearity over the full composition range and finds that the overall reaction order is 0.95, consistent with expectations for a first-order process. In contrast, data in hexadecane are nonlinear, and we observe an apparent order of 1.3, despite generating the data via simulation of a first order reaction. The reason that we observe linearity in the water data set is that, for concentrations from 0.01 to 2.0M, reactant mole fractions range from 10^{-4} to 0.05 in water. Thus, all aqueous-phase reaction rates are calculated at or near the infinite dilution limit, where activity coefficients are insensitive to composition. In contrast, for reactant concentrations of 0.01 to 2.0M in hexadecane, reactant mole fractions vary from 0.003 to 0.42. The upper end of this range falls well outside the infinite dilution limit, and activity coefficients (and thus rate constants) change dramatically with reactant concentration in hexadecane. Hence, we observe non-first order behavior for a process that is fundamentally first order.

Considering data obtained only at and below a concentration of 0.1M (Figure 3b) in each solvent, we observe approximately first-order kinetics in both cases because, at and below 0.1M, both water and hexadecane systems are sufficiently close to the infinite dilution limit that activity coefficients are composition-independent. In contrast, isolating high concentration data ($C_j \geq 0.2$M) we observe a 0.9 order in water alongside a 1.7 order in hexadecane. Even at high concentrations, the aqueous system remains relatively close to infinite dilution, but the organic system does not; hence, rate constants have a strong composition dependence in the latter, and one observes a corrupted reaction order.

These phenomena are notable because our usual tendency is to interpret significant changes in reaction order as evidence of distinct mechanisms or rate controlling steps, but they may also arise simply from a composition-dependent impact of solvation. Such solvent-induced changes in reaction order (without a change in the underlying mechanism or rate determining step) have been observed experimentally during the etherification of 5-hydroxymethylfurfural with ethanol in an ethanol/water solvent system [22]. Predicting these composition-dependent solvation effects *a priori* can be difficult because the relationship between concentration and mole fractions differs among solvents, and the impact of composition on activity coefficients is both complex and solvent-specific. In reality, many experimental systems likely move into or out of the infinite dilution limit upon variation in solvent identity and/or solute concentration; however, the resulting thermodynamic non-idealities are generally not addressed. Considering this, best practice in the analysis of solvation effects is to control species mole fractions instead of concentrations and to maintain systems at conditions where activity coefficients (and therefore rate constants) are composition-independent. This is best accomplished by operating at or near infinite dilution ($x_A < 0.01$). While activity coefficients are also nearly invariant close to the pure species limit ($0.9 \leq x_A \leq 1.0$), it is not generally possible to obtain a meaningful reaction order in that regime since changes in solute concentration at the pure species limit are too small to produce a statistically significant response in the rate of reaction. If solute mole fractions vary between $0.01 \leq x_A \leq 0.90$, one should assume that activity coefficients are strongly composition-dependent and, as highlighted in the case of 2-pentanone in water, may vary by orders of magnitude (see the discussion of UNIFAC activity coefficients in Section 2.3).

4.1.4 Activity-based Rate Expressions

Because thermodynamic activities enable a rigorous description of chemical potential, it is tempting to simply replace composition-based, mass-action rate expressions for elementary steps with their activity-based analogs (*e.g.*, $r = ka_A$ instead of $r = kC_A$); we caution against doint this without forethought. According to Transition State Theory, reaction rates scale with the number of transition states, not their thermodynamic activities. Thermodynamic activities appear in elementary rate expressions because of the assumption that the transition state is in equilibrium with the initial state, and one cannot avoid the activity coefficient for the transition state simply by writing an activity-based mass-action statement. As an illustration, we compute reaction rates as a function of reactant activity using Eq. 24 and assuming $k^\circ = 1.0$. We note that the product $\gamma_A x_A$ appearing in Eq. 24 is equal to the activity of species A in solution. As before, we use the Margules model to capture the impacts of reactant and transition state solvation. This analysis makes clear that an activity-based expression is rigorous only if the transition state is not solvated (Figure 4a). Otherwise, the (composition-dependent) activity coefficient for the transition state will lead to nonlinearity as shown in Figure 4b. Writing rate expressions based on reactant activity alone neglects the contribution of transition state solvation; therefore, it is best practice to initiate development of elementary rate expressions in consideration of the number of transition states in a system and to retain activity coefficients for reactants and transition states unless chemical intuition or computational data suggest that they are of comparable magnitude and will cancel from the rate expression.

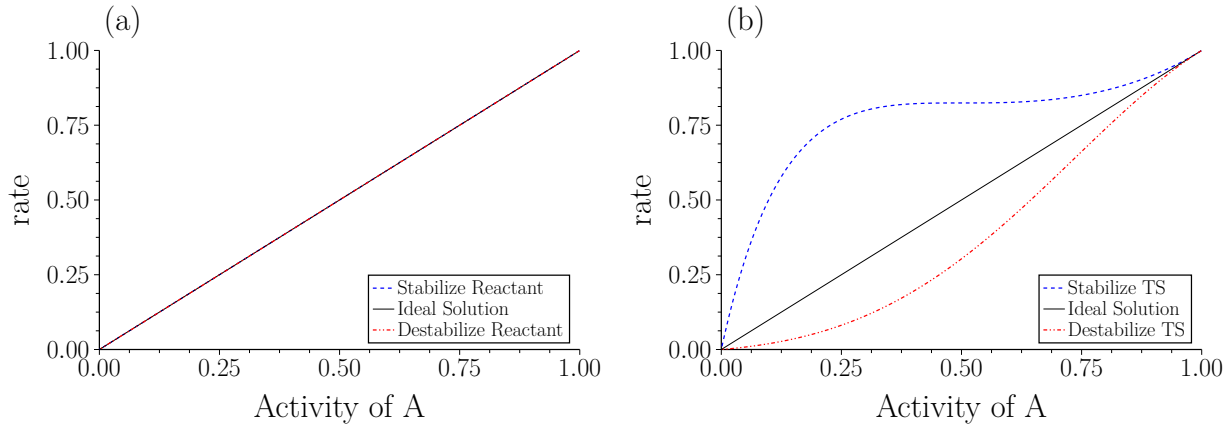

Figure 4: (a) Reaction rates are linear with respect to thermodynamic activity when $\gamma^\ddagger = 1$, and (b) non-linear when the transition state is solvated. $k^\circ = 1.0$; Ideal Solution, $\Lambda_{j,S} = 0$ (——); Stabilization, $\Lambda_{j,S} = -2$ (– – –); Destabilization, $\Lambda_{j,S} = 2$ (– · · –).

4.2 Reversible Reactions

The effects of solvation become increasingly complex as we transition to the more general case of a reversible elementary step:

$$A \rightleftharpoons B$$

In short, one must now consider how solvation impacts both rate and equilibrium constants, *i.e.*, the kinetic and thermodynamic drivers for reaction.

4.2.1 Thermodynamic vs. Kinetic Solvent Effects

Here, we characterize the impacts of changing rate constants and reaction affinity through consideration of a reversible, liquid-phase elementary step, $A \rightleftharpoons B$. We again illustrate outcomes observed in a constant volume batch reactor. We introduce an external solvent, S, which does not participate in the reaction and solvates either the transition state, $A^{\ddagger}$, or the reaction product, B, without solvating the reactant, A. We isolate kinetic and thermodynamic impacts by separately considering solvation of the transition state and the product. As before, we employ a single-parameter Margules model, where activity coefficients are determined entirely by the solvent mole fraction. We consider three cases: thermodynamic ideality ($\Lambda_{j,S} = 0$), stabilization ($\Lambda_{j,S} = -2$), and destabilization ($\Lambda_{j,S} = 2$). Further, we ensure that the solvent, S, is present in large excess ($x_S = 0.999$), and that mole fractions for species A and B are always maintained in the infinite dilution limit ($x_A \approx x_B \leq 0.001$). This ensures that activity coefficients, while deviating substantially from unity, are always composition-independent. Finally, we compute the rate of reaction using Eq. 35, and we fix the standard state rate and equilibrium constants (k°, K°) to values of 1.0.

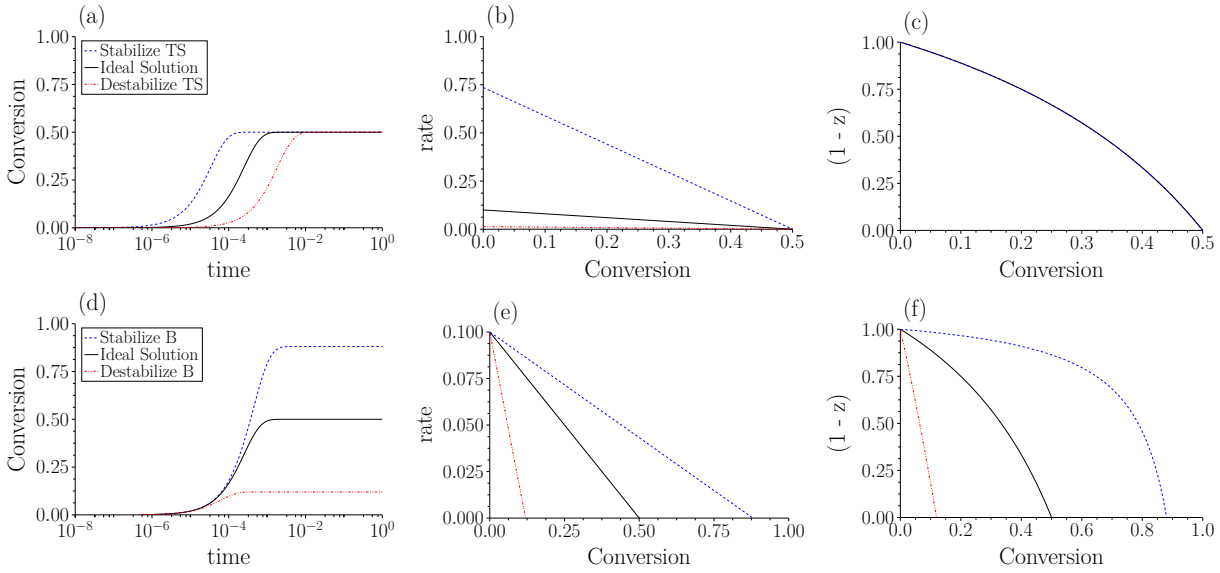

Figure 5: Combined kinetic and thermodynamic impacts of solvation; $k^{\circ} = 1.0$, $K^{\circ} = 1.0$. (a-c, top row) show the impacts of solvation on the forward rate constant, while (d-f, bottom row) show the impacts of solvation on reaction affinity. Ideal Solution, ($\Lambda_{j,S} = 0$) (——); Stabilization, ($\Lambda_{j,S} = -2$) (– – –); Destabilization, ($\Lambda_{j,S} = 2$) (– · · –).

The top panel in Figure 5 illustrates the impacts of solvating the transition state. As in consideration of the irreversible reaction, one observes that stabilizing the transition state accelerates completion of the reaction (Figure 5a), while destabilization achieves the opposite. Importantly, the change in excess free energy of *reaction* for this case is zero, and the system always achieves the equilibrium conversion anticipated in a thermodynamically ideal system

(50%). The kinetic impact of changing the solvent is evident in Figure 5b. The rate of reaction observed in the zero conversion limit (y-intercept) represents the forward rate of reaction at zero conversion; it is increased by stabilizing the transition state and decreased by destabilizing the transition state. Finally, Figure 5c shows that the thermodynamic driving force for reaction, $(1 - z)$, is independent of transition state solvation as expected for an elementary step.

We next consider impacts of solvation-induced changes in the excess Gibbs free energy of reaction (Figures 5d - f). Changes to the reaction free energy should manifest as changes in the equilibrium conversion, which are clearly observed in Figure 5d: stabilizing the reaction product increases equilibrium conversion while destabilizing the product decreases equilibrium conversion. Less intuitive is that each system reaches equilibrium on different time scales (note the logarithmic X-axis). This indicates that product solvation impacts reaction kinetics without perturbing the transition state.[5] As shown in Figure 5e, reaction rates vary as a function of fractional conversion; however, because the transition state is not solvated, the rate at zero conversion is unperturbed by solvation, and all systems have a common y-intercept of 0.10. This y-intercept represents the rate of reaction at infinite displacement from chemical equilibrium. It is a purely "kinetic" term, so it is independent of reaction free energy. As conversion increases, the thermodynamic driving force decays in all cases, but we observe substantial variation with the solvent environment. This arises through a perturbation to the reversibility, which is clearly demonstrated in Figure 5f, where stabilization and destabilization of the product have a dramatic effect on the thermodynamic driving force. In the case of product stabilization, there is no meaningful change in reversibility below $\approx 25\%$ conversion, whereas destabilizing the reaction product causes the system to reach equilibrium ($z = 1$) at $\approx 10\%$ conversion. That reaction rates can be so dramatically impacted even at low conversion ($< 5\%$) suggests that care must be taken to measure forward reaction rates at true differential conditions, which must be determined based on knowledge of the reaction equilibrium (as is routinely done, for example, when studying the water-gas shift or ammonia synthesis reactions in the gas phase). Unfortunately, this can be challenging in liquid media because, while activity coefficients can be calculated, they are not tabulated. In cases where one is uncertain of the equilibrium limit, best practice is to measure conversion and product yields at multiple residence times. In the differential limit, conversion and yield will increase linearly with residence time, and the slope of the observed trend provides a good estimate of the forward rate of reaction.

[5]For the sake of a holistic interpretation, it is worth considering that stabilization and destabilization of the reaction product constitutes a change in the free energy difference between the product and the transition state, i.e., the free energy of activation for the reverse step. From the perspective of the reverse reaction, this is a "kinetic" effect using our own terminology. Despite this, we categorize it as a "thermodynamic" effect since the free energy separation between the transition state and the reactant remains fixed in this scenario. Specifically, we classify this as a change in the reversibility of the forward reaction.

5 Using De Donder Relations to Analyze Multi-step Reaction Mechanisms

We next consider a common scenario in catalytic kinetics: that of a multi-step mechanism that includes surface adsorption and reaction. For simplicity, we will analyze a surface-catalyzed unimolecular isomerization according to the adsorption-reaction sequence shown below.

$$\begin{array}{ll} 1. & A + * \rightleftharpoons A_* \\ 2. & A_* \rightleftharpoons B + * \\ & \hline \\ & A \rightleftharpoons B \end{array}$$

Here, solvation effects become non-intuitive. The effects on a single elementary step illustrated in the prior case studies still hold, but they are convoluted with effects on additional elementary steps in the reaction sequence. For example, using our own terminology, stabilizing the surface intermediate, A_*, in isolation has a "thermodynamic" effect on the first elementary step (solvation of the product relative to the reactant), whereas, with respect to the second step, it has both "thermodynamic" effects (solvation of the reactant relative to the product) and "kinetic" effects (solvation of the reactant relative to the transition state). Accordingly, it is difficult to predict how solvation of individual species will manifest in a multi-reaction sequence. To facilitate visualization, we first develop an overall rate expression, and we subsequently plot outcomes anticipated in a batch reactor.

Following the approaches described in Section 3, one can derive expressions for the turnover frequencies of steps 1 and 2 (see Appendix B); here, the triple-prime notation denotes dimensions of inverse time:

$$r_1''' = k_1^\circ \frac{\gamma_A \gamma_*}{{\gamma_1}^\ddagger} \cdot x_A \theta_* \left(1 - \frac{1}{K_1^\circ} \frac{\gamma_{A_*}}{\gamma_A \gamma_*} \frac{\theta_A}{x_A \theta_*} \right) \tag{40}$$

$$r_2''' = k_2^\circ \frac{\gamma_{A_*}}{{\gamma_2}^\ddagger} \cdot \theta_A \left(1 - \frac{1}{K_2^\circ} \frac{\gamma_B \gamma_*}{\gamma_{A_*}} \frac{x_B \theta_*}{\theta_A} \right) \tag{41}$$

We consider the case where the first step is fast and quasi-equilibrated, and the second step is slow and rate-controlling. Assuming a Langmuirian surface, we solve for the coverages of vacant sites, θ_*, and adsorbed A_* species, θ_A:

$$\theta_* = \frac{1}{1 + K_1^\circ x_A \frac{\gamma_A \gamma_*}{\gamma_{A_*}}} \tag{42}$$

$$\theta_A = \frac{K_1^\circ x_A \frac{\gamma_A \gamma_*}{\gamma_{A_*}}}{1 + K_1^\circ x_A \frac{\gamma_A \gamma_*}{\gamma_{A_*}}} \tag{43}$$

Substitution of these coverages into the rate of step 2 (Eq. 41) leads to an expression for the overall reaction rate in turnover frequency units:

$$r''' = \frac{k_2^\circ}{\gamma_2^\ddagger}\left(\frac{K_1^\circ x_A \gamma_A \gamma_*}{1 + K_1^\circ x_A \frac{\gamma_A \gamma_*}{\gamma_{A_*}}} - \frac{1}{K_2^\circ}\frac{x_B \gamma_B \gamma_*}{1 + K_1^\circ \frac{\gamma_A \gamma_*}{\gamma_{A_*}} x_A}\right) \tag{44}$$

To examine the impact of solvation on the the overall $A \rightleftharpoons B$ reaction, we evaluate the case where this reaction is carried out in a constant-volume batch reactor containing 10^{-3} moles of active sites, 0.1 moles of A, and 99.9 moles of a solvent, S, that does not participate in the reaction. The initial mole fraction of A is set to 0.001 to ensure that bulk mole fractions of species A and B are always maintained in the infinite dilution limit, which guarantees conversion-independent solvation effects and allows us to isolate impacts of specific free energy perturbations. In this case, we assume that the reactant, A, and the vacant site, $*$, do not experience solvation (*i.e.*, $\gamma_A = \gamma_* = 1$). We consider only the impacts of solvating the kinetically relevant transition state, TS_2, the reaction product, B, and the surface-bound intermediate, A_*. Because we have assumed that the first reaction is quasi-equilibrated, the activity coefficient for the first transition state is absent from the overall rate expression, and its solvation has no impact on the overall rate of reaction.

In examining the overall rate expression (Eq. 44) one observes similar functional dependencies on the activity coefficient of the kinetically relevant transition state, $\gamma_2^\ddagger$, and the reaction product, γ_B, as shown in the prior example of a single elementary step, Eq. 35. It is therefore not surprising that, when stabilizing the transition state or the reaction product in step 2, one observes qualitatively similar behavior for this multi-reaction sequence to that illustrated for a single elementary step in Figure 5. Accordingly, these results are excluded as they add no new insights. The final activity coefficient that appears in the rate expression is that of the surface intermediate, A_*. Inspection of Eq. 44 suggests that impacts of solvating species A_* (*i.e.*, variation in γ_{A*}) will depend on the magnitude of K_1°, so we evaluate multiple scenarios. Reaction rates are computed using Eq. 44. For each simulation, we fix the value of k_2° at 0.01; we set the equilibrium constant of the overall reaction, $A \rightleftharpoons B$, to $K^\circ = 1.0$; and we vary the standard state equilibrium constant for the first elementary step, K_1°, from 10 to 10^5. As K_1° is varied, we calculate the equilbrium constant for the second elementary step, K_2°, as K°/K_1°. This is essential to ensure thermodynamic consistency with the overall reaction ($A \rightleftharpoons B$), which should approach an equilibrium conversion of 0.5 regardless of stabilization of the surface intermediate. Further, varying K_2° in proportion to K_1° guarantees that the thermodynamic driving force for reaction, $1 - z_2$, as a function of reaction extent is independent of solvating species A_*. Finally, we fix activity coefficients for all species other than the surface intermediate to 1.0, and we consider the cases where, relative to all other species, the surface intermediate is stabilized ($\Lambda_{A_*,S} = -2$), destabilized ($\Lambda_{A_*,S} = 2$), or experiences no solvation ($\Lambda_{A_*,S} = 0$). We assume that species A_* is exposed to the same infinite dilution environment as bulk species A and B, so we compute γ_{A_*} as a function of bulk solvent mole fraction using the single parameter Margules model.[6] As shown

[6] One can envision scenarios where surface species (including transition states) exist in a different solvent environment than the bulk species, including species present inside zeolite pores [23, 26] or in catalysts

in Figures 6 to 8, the observed behavior is non-intuitive.

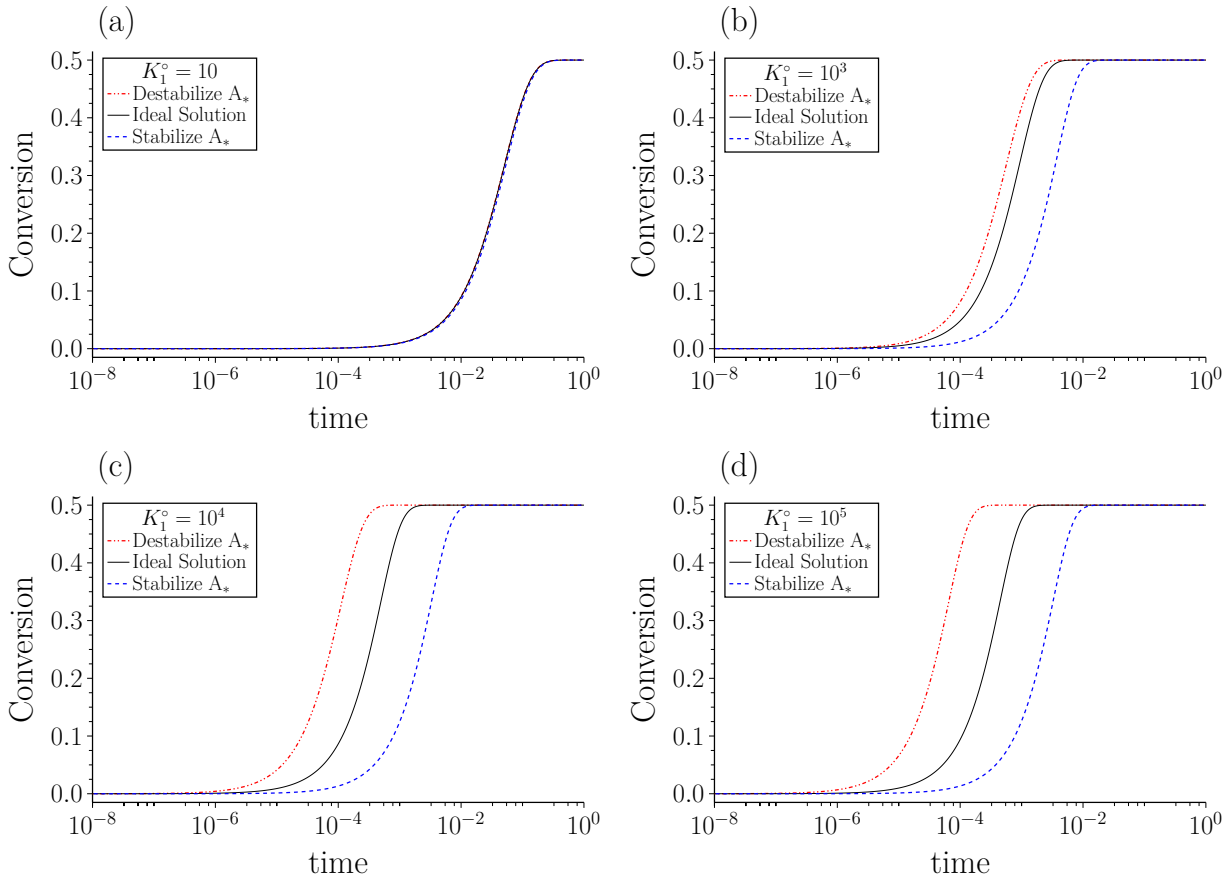

Figure 6: Fractional conversion of A as a function of time in a batch reactor upon solvation of a surface intermediate for a range of standard state adsorption equilibrium constants with $k_2^\circ = 0.01$ and $K_2^\circ = 1/K_1^\circ$. a) $K_1^\circ = 10$, b) $K_1^\circ = 10^3$, c) $K_1^\circ = 10^4$, d) $K_1^\circ = 10^5$. Ideal Solution, $\Lambda_{A_*,S} = 0$ (——); Stabilize A_*, $\Lambda_{A_*,S} = -2$ (– – –); Destabilize A_*, $\Lambda_{A_*,S} = 2$ (–·–·–).

In Figure 6, we plot fractional conversion as a function of time in a batch reactor wherein species A, B, and A_* are always present at infinite dilution and wherein species A_* experiences various solvation environments. As anticipated, the impacts of solvating A_* are extremely sensitive to the value of the standard state equilibrium constant for step 1, K_1°, and we find that the approach to an equilibrium conversion of 0.5 is impacted by solvation of A_* only for large values of K_1°. Interestingly, *stabilizing* the surface intermediate, A_*, slows the approach to equilibrium relative to the thermoydnamically ideal case, whereas *destabilizing* the surface intermediate accelerates the reaction. The underlying reason is not immediately apparent. To gain further insight, we plot surface coverages for species A_* as a function of reaction time in each solvent enviroment (Figure 7). These coverages were obtained directly from the simulations used to generate conversion profiles illustrated in Figure 6. Consistent with intuition, we find that stabilizing A_* relative to A in solution increases its

that contain microenvironments [30], among other examples [29]. The same formalism applies to these situations, and our conclusions here mirror those from the experimental works cited, although the mechanics of computing activity coefficients or excess Gibbs free energies are more complicated.

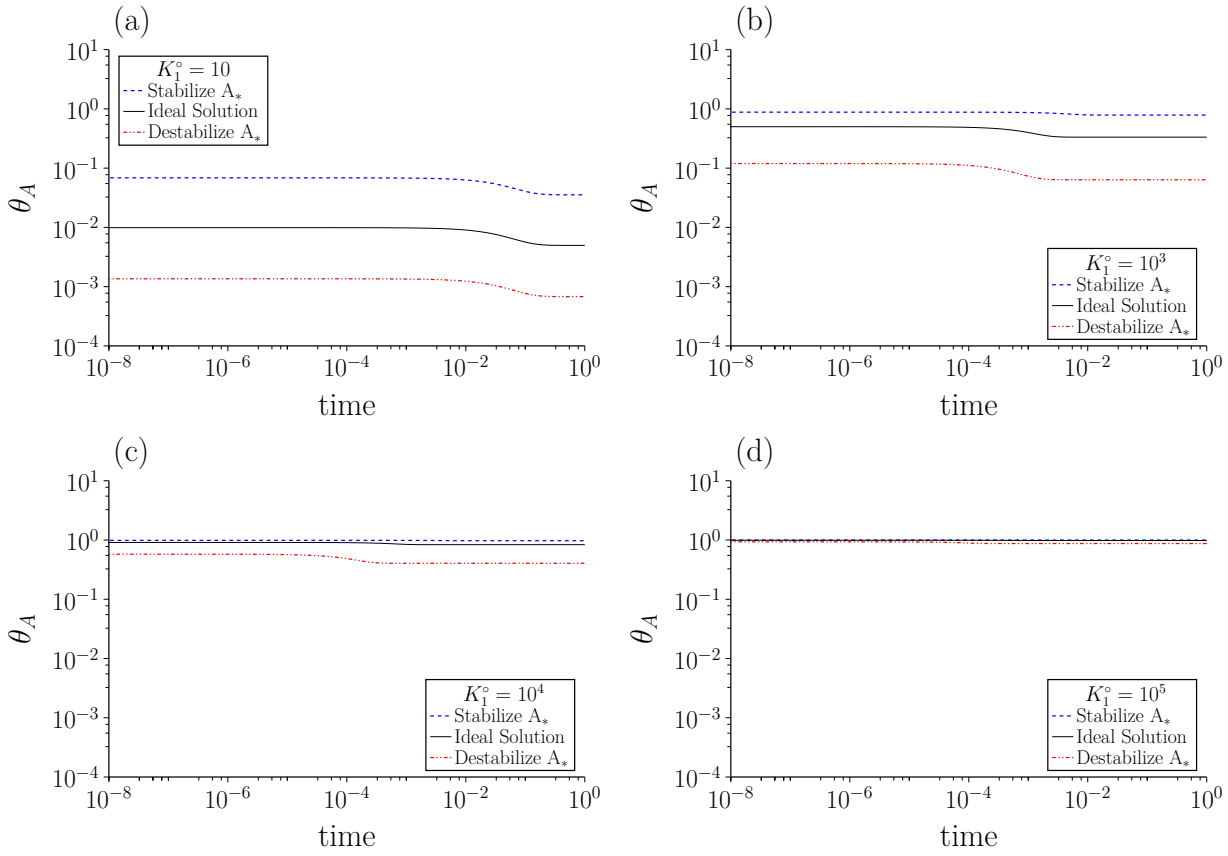

Figure 7: Coverages of A_* as a function of time in a batch reactor for solvation of a surface intermediate for a range of standard state adsorption equilibrium constants with $k_2^\circ = 0.01$ and $K_2^\circ = 1/K_1^\circ$. a) $K_1^\circ = 10$, b) $K_1^\circ = 10^3$, c) $K_1^\circ = 10^4$, d) $K_1^\circ = 10^5$. Ideal Solution, $\Lambda_{A_*,S} = 0$ (——); Stabilize A_*, $\Lambda_{A_*,S} = -2$ (– – –); Destabilize A_*, $\Lambda_{A_*,S} = 2$ (– · · –).

fractional coverage compared to the thermodynamically ideal case, whereas destabilizing it reduces coverage. This impact is most pronounced for small values of K_1°, and it diminishes as $K_1^\circ \to \infty$, where all systems approach saturation. Curiously, the correlation between solvation and coverage is exactly opposite to the correlation between solvation and fractional conversion. Specifically, we find that the time scales required to reach equilibrium are most sensitive to the solvation of A_* for large values of K_1° (Figure 6d), yet solvation of A_* has little impact on coverage in this regime (Figure 7d). In contrast, a comparison of Figure 6a and Figure 7a for the case where $K_1^\circ = 10$ shows that order-of-magnitude variations in coverage have no apparent impact on reaction rates, which is counterintuitive for a unimolecular surface reaction

The origins of these phenomena can be understood by examining trends in coverage, thermodynamic activity, and rate as a function of K_1°. Here, we compute quantities of interest at zero conversion in a system where the mole fraction of species A is 0.001, the mole fraction of species B is 0.0, and the solvent mole fraction is 0.999. We consider a range of activity coefficients for the surface intermediate, A_*, to capture stabilization ($\ln(\gamma) < 0$) and destabilization ($\ln(\gamma) > 0$). Activity coefficients were computed with a single parameter

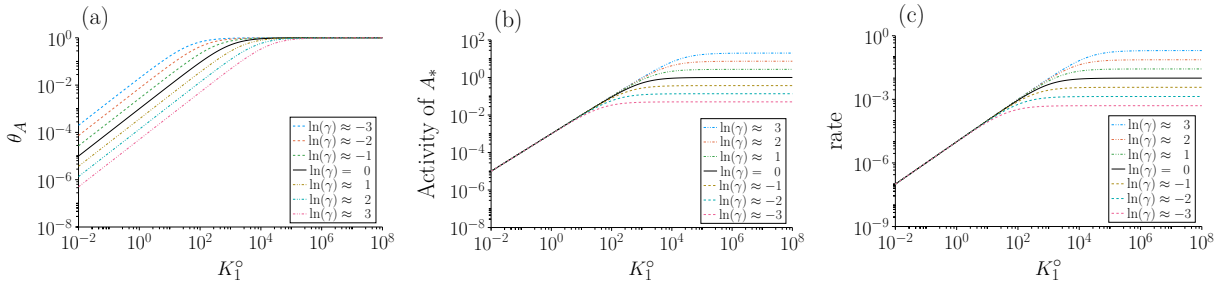

Figure 8: Trends in a) coverage, b) thermodynamic activity, and c) reaction rate upon variation in K_1°; $k_2^\circ = 0.01$. Ideal Solution (——); Stabilize A_* (– – –); Destabilize A_* (– · · –).

Margules model with coefficients, $\Lambda_{A_*,S}$, ranging from -3 to 3 at a solvent mole fraction of 0.999, and results are presented in Figure 8. Consistent with expectations, coverages are generally higher in instances where A_* is stabilized; however, this is most prevalent for small equilibrium constants and in situations where coverages are low. As one considers increasingly large equilibrium constants, the surface coverage for all solvent environments converges to unity as required by the site balance. Consideration of thermodynamic activities reveals an interesting compensation effect (Figure 8b). Specifically, for values of $K_1^\circ < 10 - 100$ we observe identical activities for species A_* in all solvent environments despite considerable variation in coverage. Although destabilization of the surface intermediate decreases its coverage, it also increases its activity coefficient, resulting in a constant thermodynamic activity for the surface intermediate. In contrast, the maximum attainable surface coverage is 1.0, but activity coefficients change considerably from one solvent to the next; hence, we see pronounced differences in thermodynamic activity (*i.e., reactivity*) at high coverage. This can be rationalized by considering that the activity for species A_* is given by:

$$a_{A*} = \gamma_{A_*}\theta_A \tag{45}$$

And at low coverages:

$$\theta_A \approx K_1^\circ x_A \frac{\gamma_A \gamma_*}{\gamma_{A_*}} \tag{46}$$

Writing the activity of A_* by combining Equations 45 and 46, we see a cancellation of the activity coefficient for species A_*; thus, at low coverages, its thermodynamic activity is independent of solvation and directly proportional to the mole fraction of species A in solution. For this reason, we observe comparable reaction rates and thus fractional conversions in cases of stabilization, destabilization, and thermodynamically ideal media for small values of K_1° (Figure 6a). In contrast, in the high coverage limit, we find:

$$\theta_A \approx 1 \tag{47}$$

Here, the thermodynamic activity of A_* is equal to its activity coefficient per Eq. 45. For this reason, the thermodynamic activity for A_* under saturation conditions is higher when

it is destabilized relative to the bulk ($\ln(\gamma_{A_*}) > 0$) and lower when it is stabilized relative to the bulk ($\ln(\gamma_{A_*}) < 0$). Essentially, under saturation conditions observed at high values of the equilibrium constant, the destabilized surface intermediate is "more reactive" because the free energy separation between it and the transition state of the kinetically relevant step, TS_2, is diminished relative to the thermodynamically ideal environment. This result is apparent if one examines the overall rate expression, Eq. 44, at low coverage regimes. Because the simulations underlying Figure 8 were performed at zero conversion, we neglect the contribution of the reverse reaction to find:

$$r''' = k_2^\circ K_1^\circ \frac{\gamma_A \gamma_*}{\gamma_2^\ddagger} \tag{48}$$

It is clear from this expression that the overall reaction rate at low coverage depends on the differential solvation between the bulk reactant, A, and the kinetically relevant transition state, TS_2. Thus, it is independent of the degree of solvation for the surface intermediate. In contrast, in the high coverage regime, the overall rate depends on the degree to which the surface intermediate, A_*, is solvated relative to the kinetically relevant transition state, TS_2:

$$r''' = k_2^\circ \frac{\gamma_{A_*}}{\gamma_2^\ddagger} \tag{49}$$

In this case, the rate of reaction scales directly with the activity coefficient for the surface intermediate; hence, we observe larger reaction rates and a more rapid increase in fractional conversion for the case of a destabilized surface intermediate ($\gamma_{A_*} > 1$).

6 Degree of Rate Control

As the preceding examples make clear, solvation can have significant impacts on rates of reaction. Changes in excess free energies of activation manifest as changes in rate constants, so it is plausible that kinetic impacts of solvation could alter the degree of rate control in a multistep mechanism. In addition, Dumesic has demonstrated that the reversibility of an elementary step is an indicator of its kinetic significance [40, 41], and collections of reversibilities can be used to estimate degrees of rate control [42, 43, 50]. Solvation can impact reaction affinity by perturbing reversibility, potentially driving an elementary step either to equilibrium or a large displacement therefrom. Indeed, a thermodynamically rigorous interpretation of experimental results from hydrogenation studies in the presence of polymer microenvironments indicates that adsorption equilibrium constants can be impacted enough by solvation to meaningfully alter the coverage of abundant surface species [30]. Thus, one may posit that Degree of Rate Control can be influenced by both thermodynamic and kinetic effects of solvation. As discussed in the preceding example, the convoluted impacts of solvation on multi-step reactions are difficult to anticipate, so we present them in the context of a simple example. Specifically, we consider the surface-mediated isomerization reaction outlined in Section 5 under identical conditions of infinite dilution of species A in solvent S. To facilitate analysis of rate control, we relax the assumption that adsorption is

equilibrated, and we instead consider the process at steady state in a CSTR. In this case, one can derive an overall rate expression by considering that the coverage of the surface intermediate, A_*, is time invariant. For simplicity, we restrict consideration to the zero-conversion limit, where the product mole fraction, x_B, is equal to zero. Ultimately, we arrive at Eq. 50 (See Appendix B).

$$r''' = \frac{k_1^\circ k_2^\circ \frac{\gamma_A \gamma_* \gamma_{A_*}}{\gamma_1^\ddagger \gamma_2^\ddagger} x_A}{\frac{k_1^\circ}{K_1^\circ}\frac{\gamma_{A_*}}{\gamma_1^\ddagger} + k_2^\circ \frac{\gamma_{A_*}}{\gamma_2^\ddagger} + k_1^\circ \frac{\gamma_A \gamma_*}{\gamma_1^\ddagger} x_A} \tag{50}$$

As developed by Campbell, the degree of rate control for each step is given by:

$$X_{RC_i} = \frac{k_{f,i}}{r}\frac{\partial r}{\partial k_{f,i}}\bigg|_{K_i, k_j \neq i} \tag{51}$$

In this equation, $k_{f,i}$ and K_i are, respectively, the forward rate constant and the equilibrium constant for the i^{th} step in the reaction mechanism. Importantly, K_i must be held constant when differentiating with respect to $k_{f,i}$, which requires that reverse rate constant for step i also change upon differentiation. We ensure this by defining reverse constants using Eq. 5. Rate constants for all remaining steps ($i \neq j$) are also held constant during analysis of the i^{th} step. Finally, r is the overall rate of reaction, which can be calculated either using Eq. 50 or by numerically integrating the transient CSTR balance on A_* until reaching steady state. We used the latter approach to estimate the degree of rate control for step 1, X_{RC_1}, by subjecting the system to a 0.1% change in k_1°. The resultant change in reaction rate was used to approximate the derivative in Eq. 51, allowing us to quantify X_{RC_1} in various solvation environments and parameter spaces. Specifically, inspection of Eq. 50 suggests that the overall reaction rate (and thus, potentially, the Degree of Rate Control) is sensitive to k_1°, k_2°, and K_1°. Accordingly, we consider a large span of values for each of these parameters in our analysis. In all scenarios, standard state rate parameters were adjusted to give $X_{RC_1} = 0.5$ in a thermodynamically ideal environment. In Figure 9, we plot X_{RC_1} for select parameter sets upon solvation of the bulk reactant, A, the surface intermediate, A_*, the reaction product, B, and the transition state for each elementary step. Varying degrees of solvation for each species are given by the magnitude of the activity coefficient, which is plotted on the x-axis. Activity coefficients were calculated using the single parameter Margules model for a solvent mole fraction of 0.999 with coefficients, $\Lambda_{j,S}$, varying from -4 to 4. Because these simulations were performed in the zero-conversion limit, the mole fraction of species B is always 0.0. Accordingly, step 2 is infinitely displaced from equilibrium, and solvation of species B has no impact on Degree of Rate Control

As illustrated in Figure 9, the extent to which solvation of a particular species affects degree of rate control depends strongly on the magnitude of standard state rate and equilibrium constants. We examine the nature of that dependence by developing an analytical solution for the Degree of Rate control for Step 1:

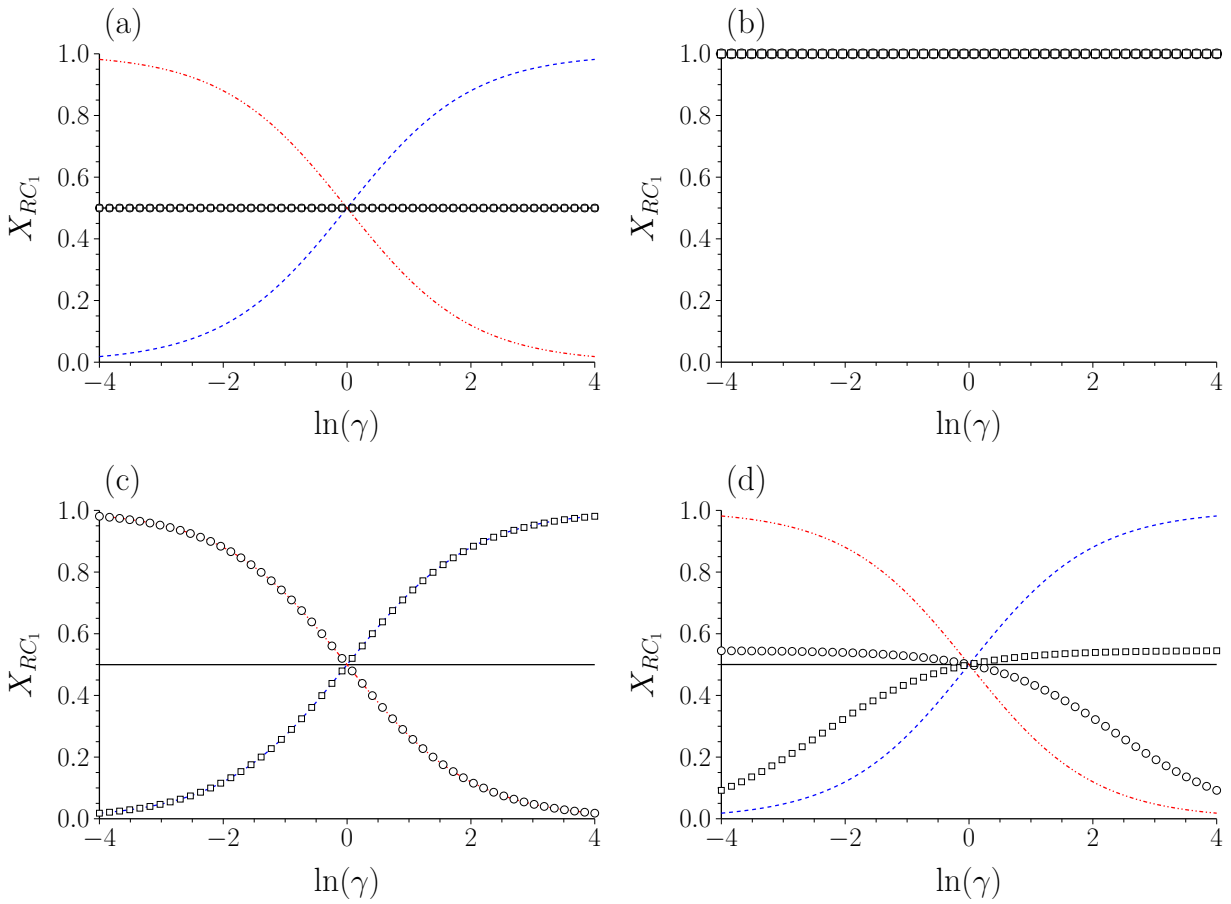

Figure 9: Impact of species solvation on degree of rate control in a 2-step reaction for various values of standard state rate and equilibrium constants a) $k_1^\circ = 0.1$, $k_2^\circ = 100$, $K_1^\circ = 0.001$, b) $k_1^\circ = 10^{-4}$, $k_2^\circ = 1.0$, $K_1^\circ = 1.0$, c) $k_1^\circ = 10^3$, $k_2^\circ = 1.0$, $K_1^\circ = 10^6$, d) $k_1^\circ = 166.5$, $k_2^\circ = 1.0$, $K_1^\circ = 200$. Solvate A (○) ; Solvate A_* (□) ; Solvate B (——); Solvate TS_1 (– – –); Solvate TS_2 (– · · –).

$$X_{RC_1} = \frac{\frac{k_2^\circ}{k_1^\circ}\frac{\gamma_{A_*}}{\gamma_2^\ddagger}}{\frac{1}{K_1^\circ}\frac{\gamma_{A_*}}{\gamma_1^\ddagger} + \frac{k_2^\circ}{k_1^\circ}\frac{\gamma_{A_*}}{\gamma_2^\ddagger} + \frac{\gamma_A}{\gamma_1^\ddagger}\mathrm{x}_A} \tag{52}$$

From this expression, we can examine the impact of solvation on degree of rate control in several regimes. First, in the limiting case where K_1° is extremely small, the leading term in the denominator will dominate, resulting in the following expression for X_{RC_1}:

$$X_{RC_1} = \frac{k_2^\circ K_1^\circ}{k_1^\circ}\frac{\gamma_1^\ddagger}{\gamma_2^\ddagger} \tag{53}$$

This corresponds to the scenario in Figure 9a, where we see that degree of rate control is only influenced by solvation of the transition states for each of the elementary steps. As the transition state for step 1 is stabilized ($\ln(\gamma_1^\ddagger) < 0$), step 1 becomes less kinetically significant, which is the anticipated consequence of stabilizing a transition state (*i.e.*, the rate of that

reaction will increase). In contrast, as the transition state for the first step is destabilized ($\ln(\gamma_1^\ddagger) > 0$), we observe an increase in the degree of rate control for step 1. Again, it stands to reason since this destabilization corresponds to a decrease in the rate constant for step 1, which should increase its degree of rate control.

Another extreme to consider is that where the ratio k_2°/k_1° is very large, such that the middle term in the denominator of Eq. 52 dominates. In this case, one finds:

$$X_{RC_1} = 1 \tag{54}$$

This is consistent with intuition: as the second reaction becomes increasingly fast relative to the first reaction, the first step will be fully rate controlling, regardless of the degree to which any species is solvated. This corresponds to the scenario in Figure 9b. Next, we consider the case where K_1° is large and the ratio of k_2°/k_1° is small. In this scenario, the final term of the denominator in Eq. 52 will dominate, and one observes the following result for degree of rate control:

$$X_{RC_1} = \frac{k_2^\circ}{k_1^\circ}\frac{\gamma_{A_*}}{\gamma_A}\frac{\gamma_1^\ddagger}{\gamma_2^\ddagger}\frac{1}{\mathrm{x}_A} \tag{55}$$

In this case, one expects that degree of rate control will be sensitive to solvation of the reactant, the surface intermediate, and both transition states. This corresponds to the illustration in Figure 9c, where one observes equal and opposite sensitivities to the solvation of A and A_* as well as TS_1 and TS_2. Inspection of Eq. 55 reveals that this is a complex regime where thermodynamic effects of solvation on step 1 (γ_{A_*}/γ_A), kinetic effects of solvation on step 1 ($\gamma_1^\ddagger/\gamma_A$), and kinetic effects of solvation on step 2 ($\gamma_{A_*}/\gamma_2^\ddagger$) may all impact the degree of rate control. The case presented in Figure 9d represents an intermediate regime where there is no single term dominating the polynomial expression in the denominator of Eq. 52. In this case, solvation of the transition states has substantial influence over degree of rate control, whereas the influences of solvation of the reactant, A, and the surface intermediate, A_*, are muted.

The major takeaway is that the impacts of solvation are complex and non-intuitive for multi-step pathways, particularly in cases where no clear rate determining step exists. That said, it is straightforward to develop rate expressions with the De Donder framework, regardless of the number of elementary steps. Although the expressions are more complex, they ensure a rigorous treatment of the kinetic and thermodyanmic impacts of solvation, and their solution is routine with modern numerical methods packages. The difficulty lies in obtaining good estimates for activity coefficients or excess free energies of solvation, but the approach is general, and we propose that it could be adopted in lieu of more conventional rate expressions, particularly for the analysis of reactions in liquid media.

7 Conclusions & Recommendations

In this Mini-review, we have shown that De Donder relations can be used to rigorously describe the impacts of solvation on elementary and multi-step reaction kinetics. Using the De Donder formalism, we classify "solvent effects" into two categories—kinetic effects that impact the rate constant of the forward reaction and thermodynamic effects that impact the reaction affinity. Generalizing this framework is straightforward, and, when implemented in basic kinetic and reactor models, one observes substantial deviations from conventionally expected behavior. Surprising trends arise because activity coefficients (and the related excess Gibbs free energies) are strongly dependent on both solvent identity and system composition. This leads to rate and equilibrium "constants" that vary with solvent identity and system composition. This is an important consideration in the analysis of liquid-phase reactions. Even for the most basic system, the impacts of solvation can be significant enough to cause deviations in measurements of reaction orders and unexpected non-linearity in standard methods for extracting kinetic parameters from reactor-scale observations. The impact of composition-dependent activity coefficients on reactivity measurements is conceptually similar to the effects of a nonzero heat of reaction in an adiabatic reactor (*i.e.*, the rate constant changes over the course of the experiment), with similar attendant changes to our interpretation of the data. We have also shown that these effects are compounded for multi-step reactions, leading to non-intuitive impacts on observed rates and kinetic trends. Because solvation can impact both rate constants and reversibilities, it can affect the degree of rate control, implying that changes in solvent can, for some reactions, change the reaction mechanism or, at the very least, the rate determining step.

For analysis of liquid-phase reactions, we make several recommendations. The first is that we increasingly make use of De Donder relations, as they capture kinetic and thermodynamic impacts of solvation while enforcing thermodynamic consistency with respect to elementary rate and equilibrium constants. Further, as De Donder relations apply for any elementary reaction, it is straightforward to extend these concepts to the analysis of multi-step reaction mechanisms. A second recommendation is that we force ourselves to explicitly consider thermodynamic reference states in kinetic analysis. Whether or not it is formally acknowledged in most analyses, one must invoke a thermodynamic reference state in developing a rate expression from Transition State Theory. Failure to acknowledge reference states may lead to the development of rate expressions that violate thermodynamic consistency. In considering the impact of solvent modulation, we suggest the use of a pure component reference state because it is independent of solvent identity. Further, in this convention, all information about non-ideality is encoded in solvent-specific activity coefficients (or, equivalently, excess Gibbs free energies). In contrast, infinite dilution reference states will generally require unique standard state rate and equilibrium constants as well as activity coefficient models for each solvent. Finally, liquid-phase kinetics experiments should ideally be performed close to the infinite dilution limit. While this approach leads to activity coefficients that are large in magnitude (based on the pure component reference state), it minimizes the more problematic composition-dependence of activity coefficients.

Underlying this approach, of course, is a general adherence to the guiding principles of catalysis research set forth by Michel Boudart. His respect for kinetic and thermodynamic

rigor, and his insistence on careful measurement of reaction rates in kinetically-controlled regimes has long been an inspiration to the authors. We are honored to continue a discussion that he began over 30 years ago.

8 Materials and Methods

All simulations discussed in Case Studies were written in Julia [68], and reactor simulations were performed using DifferentialEquations.jl package [69]. Figures were generated using Plots.jl with a PGFPlotsX backend. Source codes for each case study are provided in Jupyter Notebooks at https://github.com/jqbond/XXXXX.

9 Acknowledgements

JQB acknowledges support for research in liquid-phase systems from the National Science Foundation, awards 1605114 and 1804843. TJS acknowledges support for research in liquid-phase systems from the National Science Foundation, award 1565843, from the American Chemical Society Petroleum Research Fund, award 56712DNI5, and from the US Department of Agriculture, award 2018-67010-27905.

Appendix A. Summary of Symbols and Definitions

a_j	Thermodynamic activity of species j
f_j	Fugacity of species j in a mixture
f_j°	Fugacity of species j in a reference state
h	Planck's Constant
k_B	Boltzmann Constant
k_i	Mass action rate constant of reaction i
k_i°	Standard state rate constant of reaction i
k_i'	Apparent rate constant of reaction i
r_f	Forward rate of reaction
r_i	Volumetric rate of reaction i (intensive)
r_i'''	Surface rate of reaction i (intensive)
$\bar{r}_i$	Rate of reaction i (extensive)
x_j	Mole fraction of species j
$x^\ddagger$	Mole fraction of transition state
z_i	Reversibility of reaction i
A_i	Affinity of reaction i
Λ_{12}	Margules parameter
C_j	Molar concentration of species j
$C^\ddagger$	Molar concentration of transition state
G_j°	Partial molar Gibbs free energy of species j
G_j^E	Excess Gibbs free energy of species j
$\Delta G_i^{\circ,\ddagger}$	Standard state activation free energy of reaction i
ΔG_i°	Standard Gibbs free energy of reaction i
ΔG_i^E	Change in excess Gibbs free energy of reaction i
$\Delta G_i^{E,\ddagger}$	Change in excess Gibbs free energy of activation of reaction i
ΔH	Change in enthalpy
K_i	Equilibrium constant of reaction i
$K_i^\ddagger$	Equilibrium constant describing formation of transition state of reaction i
K_i°	Standard state equilibrium constant of reaction i
N	Total number of moles
$N^\ddagger$	Number of transition states
P	Pressure
R	Universal Gas Constant
T	Temperature
V	System volume
X_j	Fractional conversion of species j
X_{j_0}	Initial fractional conversion of species j
X_{RC_i}	Degree of rate control of reaction i
γ_j	Activity coefficient of species j
$\gamma^\ddagger$	Activity coefficient of transition state
μ_j	Chemical potential of specis j
ν_j	Species stoichiometric coefficient
$\nu^\ddagger$	Frequency factor
θ_j	Fractional surface coverage of species j
ξ	Extent of reaction

Appendix B. Supplementary material

Derivation of rate expressions from transition state theory; derivation of Equation 50. Supplementary data to this article can be found online at DOI LINK.

References

[1] D. M. Alonso, J. Q. Bond, J. A. Dumesic, *Green Chemistry* **2010**, *12*, 1493–1513.

[2] T. J. Schwartz, B. H. Shanks, J. A. Dumesic, *Current Opinion in Biotechnology* **2016**, *38*, 54–62.

[3] S. Nitopi, E. Bertheussen, S. B. Scott, X. Liu, A. K. Engstfeld, S. Horch, B. Seger, I. E. Stephens, K. Chan, C. Hahn, J. K. Nørskov, T. F. Jaramillo, I. Chorkendorff, *Chemical Reviews* **2019**, *119*, 7610–7672.

[4] X. Guo, Y. Zhu, T. Ma, *Journal of Energy Chemistry* **2017**, *26*, 1107–1116.

[5] A. R. Singh, B. A. Rohr, J. A. Schwalbe, M. Cargnello, K. Chan, T. F. Jaramillo, I. Chorkendorff, J. K. Nørskov, *ACS Catalysis* **2017**, *7*, 706–709.

[6] T. S. Wesley, Y. Román-Leshkov, Y. Surendranath, *ACS Central Science* **2021**, acscentsci.1c00293.

[7] T. J. Schwartz, J. Q. Bond, *Chemical Communications* **2017**, *53*, 8148–8151.

[8] B. Girisuta, L. P. Janssen, H. J. Heeres, *Industrial and Engineering Chemistry Research* **2007**, *46*, 1696–1708.

[9] C. M. Cai, N. Nagane, R. Kumar, C. E. Wyman, *Green Chemistry* **2014**, *16*, 3819–3829.

[10] J. N. Chheda, Y. Román-Leshkov, J. A. Dumesic, *Green Chemistry* **2007**, *9*, 342–35.

[11] Y. Román-Leshkov, J. N. Chheda, J. A. Dumesic, *Science* **2006**, *312*, 1933–1937.

[12] C. Moreau, R. Durand, S. Razigade, J. Duhamet, P. Faugeras, P. Rivalier, R. Pierre, G. Avignon, *Applied Catalysis A: General* **1996**, *145*, 211–224.

[13] Y. Nakamura, S. Morikawa, *Bulletin of the Chemical Society of Japan* **1980**, *53*, 3705–3706.

[14] M. A. Mellmer, C. Sener, J. M. R. Gallo, J. S. Luterbacher, D. M. Alonso, J. A. Dumesic, *Angewandte Chemie - International Edition* **2014**, *53*, 11872–11875.

[15] M. A. Mellmer, C. Sanpitakseree, B. Demir, P. Bai, K. Ma, M. Neurock, J. A. Dumesic, *Nature Catalysis* **2018**, *1*, 199–207.

[16] R. Weingarten, A. Rodriguez-Beuerman, F. Cao, J. S. Luterbacher, D. M. Alonso, J. A. Dumesic, G. W. Huber, *ChemCatChem* **2014**, *6*, 2229–2234.

[17] S. H. Mushrif, S. Caratzoulas, D. G. Vlachos, *Physical Chemistry Chemical Physics* **2012**, *14*, 2637–2644.

[18] T. Ståhlberg, W. Fu, J. M. Woodley, A. Riisager, *ChemSusChem* **2011**, *4*, 451–458.

[19] M. Zuo, K. Le, Z. Li, Y. Jiang, X. Zeng, X. Tang, Y. Sun, L. Lin, *Industrial Crops and Products* **2017**, *99*, 1–6.

[20] O. A. Abdelrahman, H. Y. Luo, A. Heyden, Y. Román-Leshkov, J. Q. Bond, *Journal of Catalysis* **2015**, *329*, 10–21.

[21] O. Mamun, M. Saleheen, J. Q. Bond, A. Heyden, *Journal of Catalysis* **2019**, *379*, 164–179.

[22] M. C. Allen, A. J. Hoffman, T. W. Liu, M. S. Webber, D. Hibbitts, T. J. Schwartz, *ACS Catalysis* **2020**, *10*, 6771–6785.
[23] R. Gounder, A. J. Jones, R. T. Carr, E. Iglesia, *Journal of Catalysis* **2012**, *286*, 214–223.
[24] T. J. Wilke, M. A. Barteau, *Journal of Catalysis* **2020**, *382*, 286–294.
[25] D. Mei, J. A. Lercher, *AIChE Journal* **2017**, *63*, 172–184.
[26] N. Pfriem, P. H. Hintermeier, S. Eckstein, S. Kim, Q. Liu, H. Shi, L. Milakovic, Y. Liu, G. L. Haller, Bar/'ath, Y. Liu, J. A. Lercher, *Science* **2021**, *372*, 952–957.
[27] D. T. Bregante, A. M. Johnson, A. Y. Patel, E. Z. Ayla, M. J. Cordon, B. C. Bukowski, J. Greeley, R. Gounder, D. W. Flaherty, *Journal of the American Chemical Society* **2019**, *141*, 7302–7319.
[28] J. Liu, D. Hibbitts, E. Iglesia, *Journal of the American Chemical Society* **2017**, *139*, 11789–11802.
[29] R. J. Madon, E. Iglesia, *Journal of Molecular Catalysis A: Chemical* **2000**, *163*, 189–204.
[30] T. J. Schwartz, T. S. Wesley, J. A. Dumesic, *Topics in Catalysis* **2016**, *59*, 19–28.
[31] J. S. Bates, R. Gounder, *Chemical Science* **2021**, *12*, 4699–4708.
[32] T. De Donder, *L'Affinité*, Gauthier-Villers, **1927**.
[33] M. Boudart, G. Djega-Mariadassou, *Kinetics of Heterogeneous Catalytic Reactions*, Princeton University Press, **1984**.
[34] K. G. Denbigh, *The Principles of Chemical Equilibrium*, Cambridge University Press, **1981**.
[35] K. G. Denbigh, J. C. R. Turner, *Chemical Reactor Theory: An Introduction*, Cambridge University Press, **1984**.
[36] S. I. Sandler, *Chemical and Engineering Thermodynamics*, Third, John Wiley and Sons, Inc., **1999**.
[37] K. Laidler, *Chemical Kinetics*, First, Prentice Hall, **1965**.
[38] J. P. O'Connell, J. M. Haile, *Thermodynamics: Fundamentals for Applications*, Cambridge University Press, **2005**.
[39] J. A. Dumesic, D. F. Rudd, L. M. Aparicio, J. E. Rekoske, A. A. Trevino, *The Microkinetics of Heterogeneous Catalysis*, American Chemical Society Professional Reference Books, **1993**, p. 315.
[40] J. A. Dumesic, *Journal of Catalysis* **1999**, *185*, 496–505.
[41] J. A. Dumesic, *Journal of Catalysis* **2001**, *204*, 525–529.
[42] R. D. Cortright, J. A. Dumesic, *Advances in Catalysis* **2001**, *46*, 161–264.
[43] A. H. Motagamwala, J. A. Dumesica, *Proceedings of the National Academy of Sciences of the United States of America* **2016**, *113*, E2879–E2888.
[44] C. T. Campbell, *Topics in Catalysis* **1994**, *1*, 353–366.
[45] C. T. Campbell, *Journal of Catalysis* **2001**, *204*, 520–524.
[46] C. T. Campbell, *ACS Catalysis* **2017**, *7*, 2770–2779.
[47] C. Stegelmann, A. Andreasen, C. T. Campbell, *Journal of the American Chemical Society* **2009**, *131*, 8077–8082.
[48] S. Kozuch, S. Shaik, *Journal of the American Chemical Society* **2006**, *128*, 3355–3365.
[49] S. Kozuch, J. M. Martin, *ChemPhysChem* **2011**, *12*, 1413–1418.
[50] B. L. Foley, A. Bhan, *Journal of Catalysis* **2020**, *384*, 231–251.

[51] B. L. Foley, A. Bhan, *Journal of Catalysis* **2020**, *389*, 566–577.
[52] M. Boudart, *Journal of Physical Chemistry* **1983**, *87*, 2786–2789.
[53] M. Boudart, *Industrial and Engineering Chemistry Fundamentals* **1986**, *25*, 70–75.
[54] W. L. Holstein, M. Boudart, *Journal of Physical Chemistry B* **1997**, *101*, 9991–9994.
[55] M. Boudart, *Chemical Reviews* **1995**, *95*, 661–666.
[56] M. Boudart, *Kinetics of Chemical Processes*, (Ed.: H. Brenner), Butterworth-Heinemann, **1991**.
[57] R. J. Madon, M. Boudart, *Industrial & Engineering Chemistry Fundamentals* **1982**, *21*, 438–447.
[58] D. E. Mears, *Industrial & Engineering Chemistry Process Design and Development* **1971**, *10*, 541–547.
[59] J. W. Harris, A. A. Verma, J. W. Arvay, A. J. Shih, W. N. Delgass, F. H. Ribeiro, *Journal of Catalysis* **2020**, *389*, 468–475.
[60] S. Mukherjee, M. A. Vannice, *Journal of Catalysis* **2006**, *243*, 108–130.
[61] S. Mukherjee, M. A. Vannice, *Journal of Catalysis* **2006**, *243*, 131–148.
[62] D. G. Blackmond, *Angewandte Chemie International Edition* **2009**, *48*, 2648–2654.
[63] R. C. Tolman, *Proc. Nat. Acad. Sci.* **1925**, *11*, 436–439.
[64] A. Fredenslund, R. L. Jones, J. M. Prausnitz, *AIChE Journal* **1987**, *21*, 1086–1099.
[65] K. J. Laidler, M. C. King, *J. Phys. Chem.* **1983**, *87*, 2657–2664.
[66] G. M. Wilson, *J. Am. Chem. Soc.* **1964**, *86*, 127–130.
[67] H. Renon, J. M. Prausnitz, *AIChE J.* **1968**, *14*, 135–144.
[68] J. Bezanson, A. Edelman, S. Karpinski, V. B. Shah, *SIAM Review* **2017**, *59*, 65–98.
[69] C. Rackauckas, Q. Nie, *The Journal of Open Research Software* **2017**, *5*.